JOC The Journal of Organic Chemistry

pubs.acs.org/joc Article

Contribution of Solvents to Geometrical Preference in the *Z*/*E* Equilibrium of *N*-Phenylthioacetamide

Shuyi Song, Tadashi Hyodo, Hirotaka Ikeda, Kim Anh L. Vu, Yulan Tang, Erika S. Chan, Yuko Otani, Satoshi Inagaki, Kentaro Yamaguchi, and Tomohiko Ohwada*

Cite This: https://doi.org/10.1021/acs.joc.1c00801 Read Online

ACCESS | Metrics & More | Article Recommendations | Supporting Information

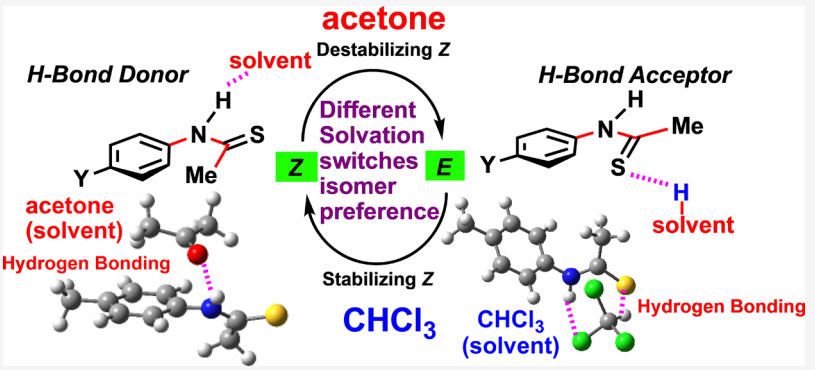

ABSTRACT: We studied the *Z*/*E* preference of *N*-phenylthioacetamide (thioacetanilide) derivatives in various solvents by means of ^{1}H NMR spectroscopy, as well as molecular dynamics (MD) and other computational analyses. Our experimental results indicate that the *Z*/*E* isomer preference of secondary (NH)thioamides of *N*-phenylthioacetamides shows substantial solvent dependency, whereas the corresponding amides do not show solvent dependency of the *Z*/*E* isomer ratios. Detailed study of the solvent effects based on molecular dynamics simulations revealed that there are two main modes of hydrogen (H)-bond formation between solvent and (NH)thioacetamide, which influence the *Z*/*E* isomer preference of (NH)thioamides. DFT calculations of NH-thioamide in the presence of one or two explicit solvent molecules in the continuum solvent model can effectively mimic the solvation by multiple solvent molecules surrounding the thioamide in MD simulations and shed light on the precise nature of the interactions between thioamide and solvent. Orbital interaction analysis showed that, counterintuitively, the *Z*/*E* preference of NH-thioacetamides is mainly determined by steric repulsion, while that of sterically congested *N*-methylthioacetamides is mainly determined by thioamide conjugation.

INTRODUCTION

The thioamide bond, which is an analogue of the amide bond, takes a planar structure due to the double-bond character of the C(S)−N bond (Figure 1),[1] and replacement of the amide carbonyl oxygen atom with a sulfur atom increases the magnitude of the bond rotation barrier. This is important because there is increasing interest in applications of thioamides, for example, to prepare peptide analogues, protein-folding probes, and synthetic intermediates.[2] Although *Z*/*E* isomerism of thioamides seems simple (Figure 2), the chemistry has been reviewed only once, in the 1970s,[3] and there are discrepancies between the review and some of the cited papers; for example, the review mentioned *Z*/*E* isomer ratios of thioamides that were not given in the original papers. Furthermore, only benzene, nitromethane, and pyridine have been investigated as solvents, in addition to chloroform.[4] While several more recent studies reported solvent dependency of thioamide rotation and *Z*/*E* ratios,[5] the chemistry of *N*-methylthioamides still needed to be updated recently.[6] Therefore, there is a need to reinvestigate the *Z*/*E* preferences

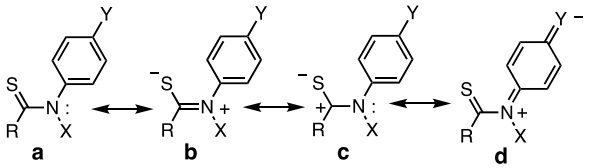

Figure 1. Thioamide resonance.

Special Issue: Solvation Effects in Organic Chemistry

Received: April 7, 2021

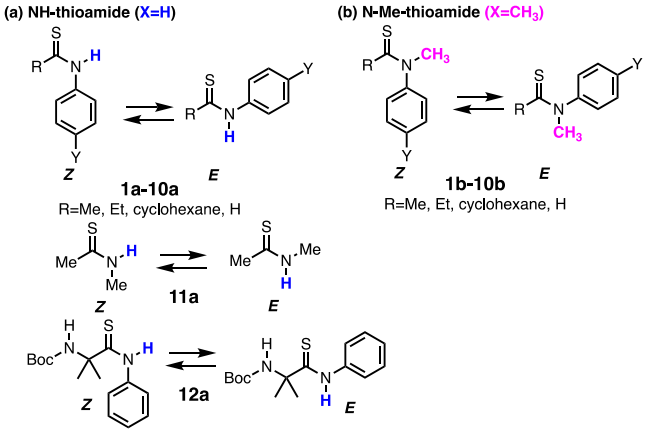

Figure 2. *Z*/*E* isomerism of *N*-phenylthioacetamide and *N*-methylthioamide.

of *N*-phenylthioacetamides (*N*-anilides), particularly the effect of solvents. In this paper, we studied the *Z*/*E* preference of various *N*-phenylthioacetamide compounds and their *N*-methyl derivatives (Figure 2 and Table 1) by means of NMR spectroscopy in standard solvent sets (Table 2).

Table 1. Substituents of *N*-Phenylthioacetamide Derivatives 1a−10a and 1b−10b[a]

compd	R	X	Y
NH-thioamide			
1a	Me	H	H
2a	Me	H	OMe
3a	Me	H	Me
4a	Me	H	Cl
5a	Me	H	F
6a	Me	H	CN
7a	Me	H	NO_2
8a	Et	H	H
9a	cyclohexyl	H	H
10a	H	H	H
N-Me-thioamide			
1b	Me	Me	H
2b	Me	Me	OMe
3b	Me	Me	Me
4b	Me	Me	Cl
5b	Me	Me	F
6b	Me	Me	CN
7b	Me	Me	NO_2
8b	Et	Me	H
9b	cyclohexyl	Me	H
10b	H	Me	H

[a]R, X, and Y are substitutents of thioamides shown in Figure 1.

We also conducted extensive molecular dynamics and other computational analyses, which indicate that the origin of the *Z*/*E* preference of NH-thioacetamides can be understood in terms of steric repulsion, while that of *N*-methylthioacetamides can be understood in terms of thioamide conjugation.

RESULTS AND DISCUSSION

Solvent Effect on the *Z*/*E* Preference of *N*-Phenylthioacetamides. The *Z*/*E* ratios of *N*-phenylthioacetamides **1a−10a** and **1b−10b** (Table 1) were evaluated from the ^{1}H NMR spectra in widely used NMR solvents, $CDCl_3$, CD_2Cl_2, acetone-d_6, CD_3OD, and DMSO-d_6. The NMR spectra of secondary thioamides (**1a−10a**), NH-thioacetamides (X = H) bearing a different aromatic substituent (Y) and those (**8a**, **9a**) bearing a different alkyl substituent (R) (Table 1) showed the signals of two isomers, which were assigned as the *E* and *Z* isomers with respect to the thioacetamides. Structural assignment of *Z*/*E* isomers of the thioacetamides were based on 2D NMR spectra analysis and GIAO calculations[7] (Figures S1−S3 and Table S1). The isomer ratio was solvent dependent (Table 2). In order to assess the effect of the hydrogen atom on the nitrogen atom (NH, X = H), we also examined the *Z*/*E* isomer preference of the *N*-methyl derivatives of *N*-phenylthioacetamides (X = Me) (**1b−10b**).

The *E* ratio of NH-thioacetamides increased as the polarity of the solvent was increased from chloroform (dielectric constant = 4.8), dichloromethane (9.1), acetone (20.6), methanol (32.6), to DMSO (47.2) (Table 2). However, there is no direct correlation between the dielectric constant of the solvent and the thioamide *Z*/*E* ratio, and the relationship is not linear: the *E* ratio was maximal in methanol but remained similar in DMSO. This trend is consistent with previous reports on the solvent dependence of rotational barriers of thioamides: the magnitude of the rotational barriers does not simply correlate with the polarity of the solvent, particularly in the cases of methanol and DMSO.[5a] As described later, we found that the conformational preferences of the *N*-phenylthioacetamides can be attributed to the hydrogen bond donor/acceptor ability of the solvent. Methanol can be considered as a hydrogen-bond-donating solvent, whereas the others are hydrogen-bond acceptors. However, our calculations showed that methanol can also work as a hydrogen-bond acceptor, probably due to the acidity difference between thioamide NH (pK_a = 18.5 for thioacetamide)[8] and methanol (pK_a = 29.0).[9]

Some NH-thioacetamides show different *Z* and *E* ratios in $CDCl_3$ and in CD_2Cl_2 (Table 2): **1a**: *Z*/*E* 45:55 ($CDCl_3$); 33:67 (CD_2Cl_2), **2a**: *Z*/*E* 47:53 ($CDCl_3$); 35:65 (CD_2Cl_2), **3a**: *Z*/*E* 49:51 ($CDCl_3$); 36:64 (CD_2Cl_2), **4a**: *Z*/*E* 31:69 ($CDCl_3$); 27:73 (CD_2Cl_2). However, in d_6-DMSO, the *E* conformer is strongly favored: **1a**: *Z*/*E* 7:93 (d_6-DMSO); **2a**: *Z*/*E* 9:91 (d_6-DMSO); **3a**: *Z*/*E* 8:92 (d_6-DMSO); **4a**: *Z*/*E* 9:91 (d_6-DMSO). Thus, aromatic substituents (**1a−7a**) appear to have relatively little effect on the *Z*/*E* isomer preference in a given solvent (Table 2), though NH-thioacetamides (**6a** and **7a**) with an electron-withdrawing group are insoluble in $CDCl_3$ and CD_2Cl_2. In the case of NH-thioamides, solvent-dependent variation in the *Z*/*E* conformer ratios seemed larger in the case of electron-rich aromatic **2a** than electron-deficient **6a** or **7a**: for example, in acetone, **2a** gave a *Z*/*E* ratio of 12:88, while **6a** and **7a** give practically only the *E* conformation (1>:>99). This is consistent with the involvement of hydrogen bonding of the acidic NH proton of the NH-thioamides in the solvent effect (*vide infra*); that is, **6a** and **7a** have a more acidic NH proton that facilitates hydrogen bonding with the solvent. Furthermore, the amide **3c** corresponding to thioamide **3a** showed no solvent effect on the *Z*/*E* ratio and the predominant isomer is *E* (>99:1<) in all of the solvents studied here (**3c**, Table 2).

In the case of thioformamide **10a** (R = H) (Table 2), the major structure is *Z* by definition (see Figure 2) because the relationship of the substituent R (= H in **10a**) and the *N*-phenyl group is *Z*. The *Z* isomer predominates (**10a**: *Z*/*E* 95:5 in $CDCl_3$), suggesting that the repulsion between *n*(S)-Ph in

https://doi.org/10.1021/acs.joc.1c00801
J. Org. Chem. XXXX, XXX, XXX−XXX

Table 2. Z/E Ratios of *N*-Phenylthioacetoamides in Various Solvents[a]

compd	Z/E ratio[a]				
NH-thioamide	$CDCl_3$	CD_2Cl_2	acetone-d_6	CD_3OD	DMSO-d_6
1a	45:55	33:67	9:91	8:92	7:93
2a	47:53	35:65	12:88	10:90	9:91
3a	49:51	36:64	11:89	9:91	8:92
4a	31:69	24:76	6:94	5:95	9:91
5a	34:64	27:73	7:93	6:94	7:93
6a	*b*	*b*	<1:>99	<1:>99	<1:>99
7a	*b*	*b*	<1:>99	<1:>99	<1:>99
8a	25:75	<1:>99	<1:>99	<1:>99	<1:>99
9a	10:90	<1:>99	<1: > 99	<1:>99	<1:>99
10a	95:5	95:5	90:10	88:12	90:10
11a	3:97	4:96	2:98	<1:>99	<1:>99
12a	3:97	4:96	2:98	<1:> 99	<1:>99
(amide) **3c**	<1:>99	<1:>99	<1:>99	<1:>99	<1:>99
NMe-thioamide					
1b	>99:<1	>99:<1	>99:<1	>99:<1	>99:<1
2b	>99:<1	>99:<1	>99:<1	>99:<1	>99:<1
3b	>99:<1	>99:<1	>99:<1	>99:<1	>99:<1
4b	>99:<1	>99:<1	>99:<1	>99:<1	>99:<1
5b	>99:<1	>99:<1	>99:<1	>99:<1	>99:<1
6b	>99:<1	>99:<1	>99:<1	>99:<1	>99:<1
7b	>99:<1	>99:<1	>99:<1	>99:<1	>99:<1
8b	>99:<1	>99:<1	>99:<1	>99:<1	>99:<1
9b	>99:<1	>99:<1	>99:<1	>99:<1	>99:<1
10b	>99:<1	>99:<1	>99:<1	>99:<1	>99:<1
11b	>99:<1	>99:<1	>99:<1	>99:<1	>99:<1

[a]At 298 K. See structures shown in Figure 1. Ratio values of <1:>99 or >99:< 1 indicate that practically only one rotamer can be observed. [b]The NMR spectrum could not be measured due to low solubility.

the *E* conformation is larger than that between *n*(S)-H(N) in the *Z* conformation, or that the repulsion between R (= H)-H(N) in the *E* conformation is larger than that between R (= H)-Ph in the *Z* conformation. This is consistent with the result of the bond model analysis of **1a** in the present work (see Figure 10 and Table S2(1)). In the case of thioformamide **10a**, solvent dependence of the Z/E ratio was also observed, and the trend is consistent with that of other NH-phenylthioacetamides **1a**−**9a**: from $CDCl_3$ and CH_2Cl_2 to CD_3OD through acetone-d_6, the *E* ratio increased slightly (5% to 10% and 12%).

The solvent dependence of the Z/E preference of NH-phenylthioacetamides **1a**−**10a** arises from the involvement of the interaction between the methyl (or alkyl R) group attached to the thiocarbonyl carbon atom, and the *N*-phenyl group.

*Rotational Barriers of **3a**.* We also measured the rotational barriers of thioamide **3a** in $CDCl_2CDCl_2$ (we need a higher boiling point solvent than $CDCl_3$) and in DMSO-d_6 by means of the coalescence method: in $CDCl_2CDCl_2$, coalescence temperature T_c = 107.2 °C (380 K) $\Delta G_c^{\ddagger}$ = 18.2 kcal/mol; in DMSO-d_6, T_c = 72.9 °C (346 K) $\Delta G_c^{\ddagger}$ = 18.7 kcal/mol. The rotational barrier of **3a** in polar DMSO-d_6 is larger than that in $CDCl_3$, which is consistent with the report on *N*,*N*-dimethylthioacetamide.[5a] However, the previous report did not clearly address the reason for these phenomena.[5a] In $CDCl_2CDCl_2$, we also analyzed the dynamic NMR to obtain the rotational barrier from the *E* form to the TS and that from the *Z* form to the TS: $\Delta G^{\ddagger}_{E\rightarrow TS}$ = 18.9 kcal/mol, $\Delta G^{\ddagger}_{Z\rightarrow TS}$ = 18.7 kcal/mol at 298 K (see Tables S1−4). These values are consistent with the results obtained with the coalescence method. The difference between the two rotational energies, that is, the observation that the *E* form is more stable than the *Z* form by 0.2 kcal/mol, is also consistent with the experimental ratio of the isomer, i.e., Z/E = 47:53 in $CDCl_2CDCl_2$ at 298 K, the value close to that of $CDCl_3$ (Z/E = 49:51, Table 2).

Effect of Alkyl Substituent (R) in N−H Phenylthioacetamides. The Z/E ratios of various N−H thioacetamide derivatives varied significantly depending on the alkyl substituent R (**1a**, **8a**, and **9a**, Table 2). For a given solvent, the ratio of the *E* isomer increased as the size of the acyl alkyl group increased from methyl (**1a**) to ethyl (**8a**) to cyclohexyl (**9a**): **1a**: *Z*:*EZ*/*E* 45:55; **8a**: Z/E 25:75; **9a**: Z/E 10:90 in $CDCl_3$. The Z/E ratio of **8a** and **9a** also changed dramatically depending upon the solvent: increasing solvent H-bond-forming ability (*vide infra*), not simply polarity, from chloroform, to dichloromethane, acetone, methanol, and DMSO leads to a sharply increased predominance of the *E* isomer (Table 2). Such a complete shift of the equilibrium to *E* thioamide was not seen in simple *N*-phenylthioacetamides (**1a**−**5a**)) (Table 2). This can be plausibly explained in terms of steric effect, i.e., the magnitude of repulsion between S and the aromatic moiety and between the acyl alkyl group and aromatic moiety may determine the Z/E ratio of thioamides.

N-Methylation of Phenylthioacetamides. *N*-Methylation of phenylthioacetamides (**1b**−**10b**) biased the Z/E equilibrium toward *Z* conformation (Table 2). All the N-Me phenylthioacetamides studied here (**1b**−**10b**) showed practically complete *Z* preference independently of the bulkiness of the acyl alkyl group, the solvent, and the aromatic substituent. This result is consistent with a recent report.[6]

A More Complicated Thioamide System. We also studied the NH-thioamide of a more complicated structure, **12a**, an

https://doi.org/10.1021/acs.joc.1c00801
J. Org. Chem. XXXX, XXX, XXX−XXX

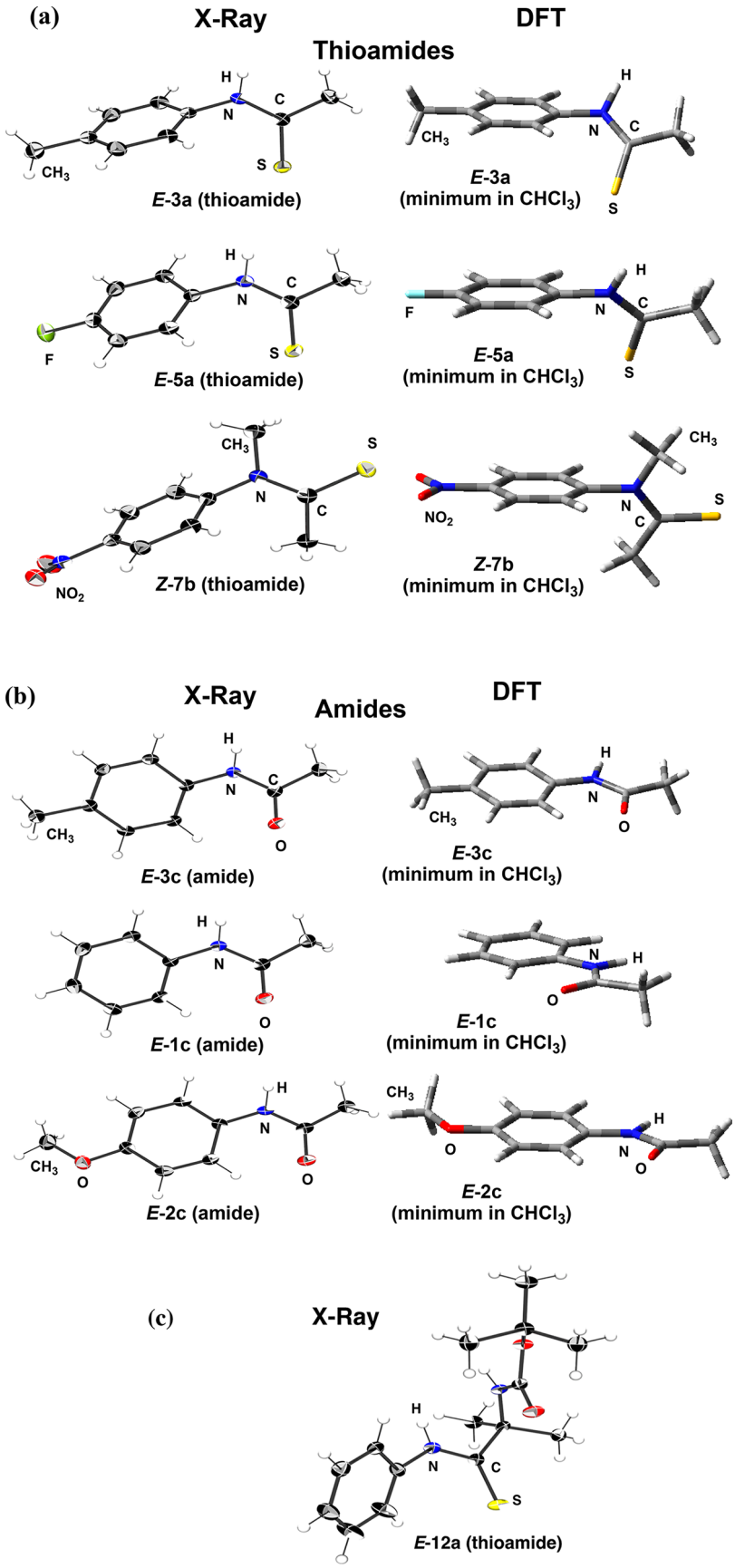

Figure 3. continued

https://doi.org/10.1021/acs.joc.1c00801
J. Org. Chem. XXXX, XXX, XXX−XXX

	C=S/O (Å)	(S/O=)C - N (Å)	N - Ar (Å)	Amide bond |ω| (°)	N-Ar torsion (°)[a]
3a (*E*)	1.674(2)	1.329(2)	1.430(2)	175.3(1)	122.9 (59.6)
5a (*E*)	1.680(2)	1.326(3)	1.426(3)	178.8(2)	124.0 (57.9)
7b (*Z*)	1.672(4)	1.341(5)	1.443(5)	5.5(6)	116.9 (65.1)
3c (*E*)	1.233(1)	1.353(1)	1.414(1)	179.1(1)	163.6 (18.1)
1c (*E*)	1.236(2)	1.356(2)	1.419(2)	175.9(1)	162.8 (17.5)
2c (*E*)	1.237(2)	1.346(2)	1.420(2)	174.4(1)	160.8 (20.0)
12a (*E*)	1.663(2)	1.334(3)	1.419(3)	173.0(2)	138.8 (39.9)
3a DFT (*E*)[b] (methanol)	1.675	1.337	1.429	178.8	121.2 (61.3)
3a DFT (*E*) [b] ($CHCl_3$)	1.664	1.341	1.427	178.1	126.4 (56.3)
5a DFT (*E*) [b] ($CHCl_3$)	1.663	1.343	1.426	178.1	124.9 (57.4)
7b DFT (*Z*) [b] ($CHCl_3$)	1.667	1.346	1.431	176.5	113.1 (68.7)
3c DFT (*E*) [b] ($CHCl_3$)	1.218	1.367	1.411	179.9	179.9 (0.2)
1c DFT (*E*) [b] ($CHCl_3$)	1.218	1.369	1.410	178.7	179.7 (0.4)
2c DFT (*E*) [b] ($CHCl_3$)	1.219	1.365	1.413	179.9	173.7 (6.9)

Figure 3. Crystal structures and related DFT structures of the *N*-phenylthioacetoamides (a), *N*-phenylacetoamides (b), and a more complexed thioacetamide **12a** (c). (a) Absolute value of the dihedral angle C−N−C(ipso)−C(ortho) is shown. The larger value is shown, with the smaller angle in parentheses. 180° (0°) indicates a planar structure of the thioamide bond with respect to the phenyl ring. (b) Optimized structures with M062X/6-311++G(d) in the PCM solvent model.

amino acid thioamide (Figure 2). Compound **12a** also favored the *E* thioamide conformer, but in halogenated solvents a small amount of *Z* conformer was observed (Table 2). Thus, the conformation is solvent-dependent, even though the magnitude of the effect is small. This solvent effect and *E* conformer preference are consistent with those of other NH-thioamides.

X-ray Crystallographic Analysis of N-Phenylthioacetamides. We next determined the crystal structures of the *E* isomers of secondary N−H thioamides **3a**[10] and the corresponding N−H amides **3c**[11] (Figure 3a, 3b and see Figures S4−S10). The *E* isomer of **3a** is the major isomer in polar solvents, and in the case of amide **3c**, the *E* isomer of **3c** is the major isomer in all the solvents studied here. In the crystal structures, the N-aromatic ring is rotated with respect to the thioamide plane in thioamide **3a**, whereas the N-aromatic ring is almost coplanar with the amide plane in amide **3c**: thioamide **3a** has a highly twisted N−Ar torsion angle (59.6°) as compared with that of the corresponding amide **3c** (18.1°). These angles represent the minimum absolute value of two possible rotational angles with respect to the Ar−N bond (Figure 3a). These results are consistent with a significant repulsive effect between the sulfur atom and the benzene ring in **3a** (*vide infra*). In **3a** and **3c**, the thioamide and amide moieties both have planar structures (see Figure 1).

The twisting of the N-aromatic ring in the thioamide was also confirmed in the crystal structure of the thioamide **5a**[12] (57.9°, Figure 3a). In the unit cell of the crystal of NH-thioamide **3a**, Hirshfeld surface analysis[13] and the 2D fingerprint[14] indicated a strong intermolecular interaction between the N−H and the sulfur atom of another molecule (Figure S4-2). Therefore, the thioamide is coordinated with another molecule in the crystal state, which is analogous to solvation in the solution state (*vide infra*). In the crystal state, the C═S bond of **3a** is longer than the C═O bond of the corresponding amide **3c** by 0.441 Å, and the N−C (═X), (X = S or O) bond in **3a** (1.329 Å) is shorter than that of the amide (**3c**, 1.353 Å). The thioamide bond of **3a** is slightly shorter than the amide bond of **3c** by 0.024 Å, and this is consistent with our DFT-optimized structural parameters (0.030 Å difference in bond length between *E* and *Z*) (*vide infra*). The coplanarity of the N-aromatic ring in the crystal structure of amide **3c** provides a sharp contrast to the corresponding thioamide **3a**. The planarity of acetamides was also confirmed in the crystal structures of other NH-phenylacetamides ((**1c**,[15] p-H) (17.5°) and (**2c**: p-OMe) (20.0°) (Figure 3b).

Finally, we are successful to obtain the crystal structure of a more complicated thioamide **12a** (Figure 3c and Figure S10). The crustal structure of **12a** is the *E* conformer, which is consistent with the *E* conformer preference in solution (Table 2). While the thioamide group takes a nonplanar structure with an *N*-phenyl group, intriguingly, the N−Ar torsion angle is rather small (39.9°) (Figure 3). This may be related to the small fraction of the *Z* conformation even in halogenated solvents (Table 2).

DFT-Optimized Structures in the Continuum Inexplicit Solvent Model. Furthermore, DFT-optimized *E* structures of thioamide **3a (p-Me)** and amide **3c (p-Me)** were obtained in the continuum solvent model (PCM) (Figure 3). We found that the minimum thioamide structure of **3a** has a twisted thioamide plane with respect to the N-benzene ring, independently of the solvent (in $CHCl_3$: 56.8° (**3a-DFT-**

https://doi.org/10.1021/acs.joc.1c00801
J. Org. Chem. XXXX, XXX, XXX−XXX

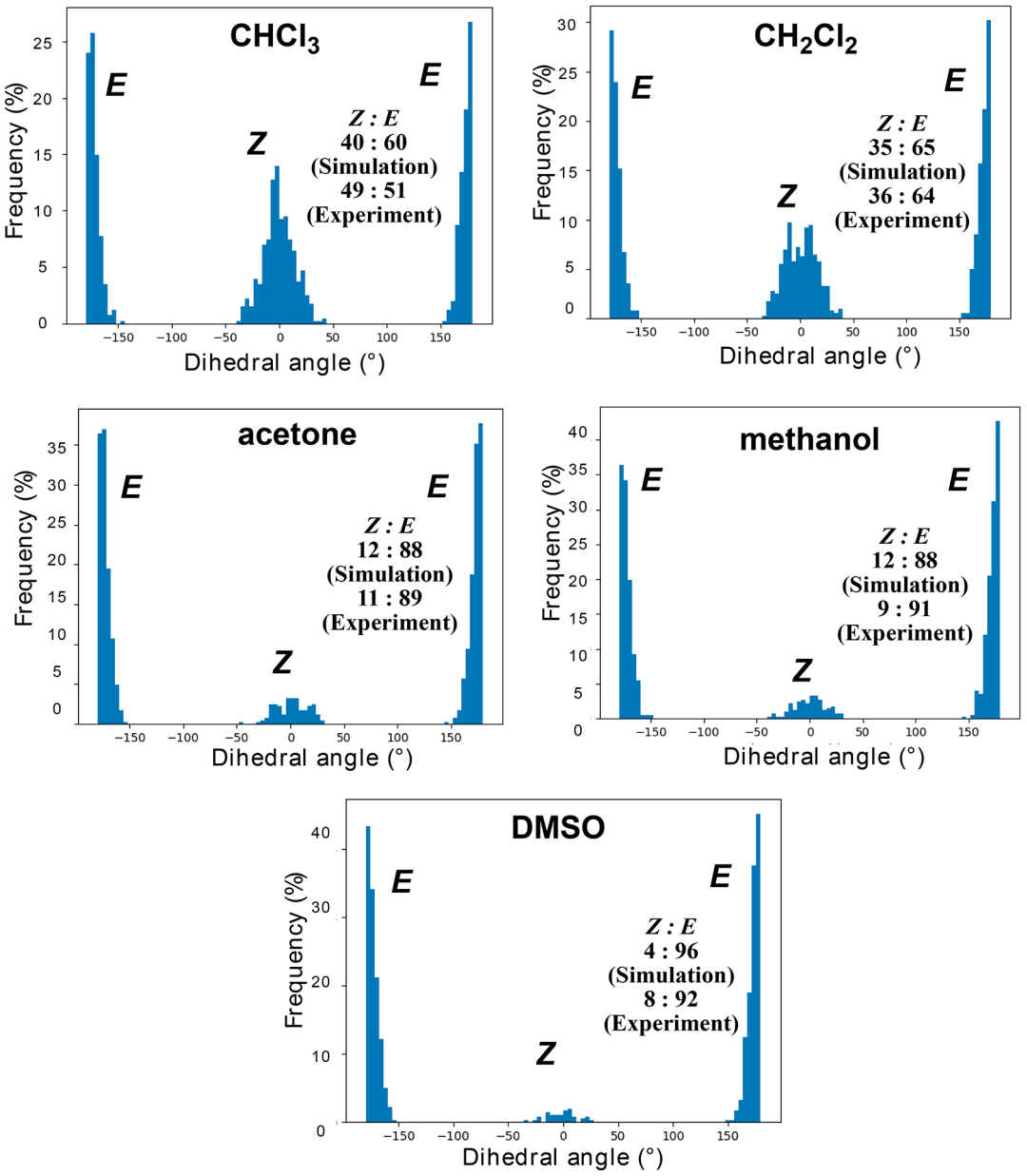

Figure 4. Distribution of *Z*/*E* isomers of NH-thioamide **3a** obtained by REST simulations at 300 K in various solvents. Horizontal axis is the dihedral angle of the thioamide rotation: conformers between −50° and +50°are regarded as the *Z* conformer and conformers between −150° to −180° and 150° to 180° are regarded as the *E* conformer. The vertical axis is the frequency of the conformer.

$CHCl_3$);in methanol: 59.6° (**3a-DFT-methanol**) (Figure 3). These calculated rotation angles are in good agreement with the experimental value in the crystal structure (**3a**, 59.6°, Figure 3). A similar rotation of the *N*-phenyl group is also found in the case of thioamide **5a** (**p-F**) (X-ray: 57.9°) and the present DFT calculation (**5a-DFT-$CHCl_3$**: 57.4°) is consistent with the experimental value. In sharp contrast, the DFT minimum structure of the corresponding amide **3a** has a coplanar relationship of the amide with the benzene ring (in $CHCl_3$: 0.3° (**3c-DFT-$CHCl_3$**)), which is also consistent with the X-ray crystal structure (**3c**, 18.1°) (Figure 3). The experimentally observed planarity of other acetamides (**1c** (17.5°) and **2c** (20.0°)) is consistent with the DFT calculation (**1c-DFT-$CHCl_3$**: 0.4°; **2c-DFT-$CHCl_3$**: 6.9°) (Figure 3). Therefore, the present experimental crystal structural data and our calculation results shown herein are all consistent with previous computational studies,[16,17] particularly for the corresponding amides, *N*-phenylacetamides. Our present X-ray crystal structure studies experimentally verify for the first time the prediction that NH-*N*-phenylacetamides tend to take a coplanar structure of the N-aromatic ring with respect to the amide, in contrast to NH-*N*-phenylthioacetamides, which take a rotated structure with respect to the *N*-phenyl group.

On the other hand, N-Me *N*-phenylthioacetamide **7b** (**p-NO_2**) takes *Z*-thioamide structure in the crystal (Figure 3), which is consistent with the *Z*-preference in solution (Table 2). The N−Ar bond of **7b** is more twisted (65.1°) than that (18.1°) of NH-*N*-phenylthioacetamide **3a**. This means that the N−Ar conjugate system and the thioamide N−C(=S) conjugate system are almost orthogonal in the N-Me *N*-phenyl thioacetamide; that is, the thioamide N−C(=S)

https://doi.org/10.1021/acs.joc.1c00801
J. Org. Chem. XXXX, XXX, XXX−XXX

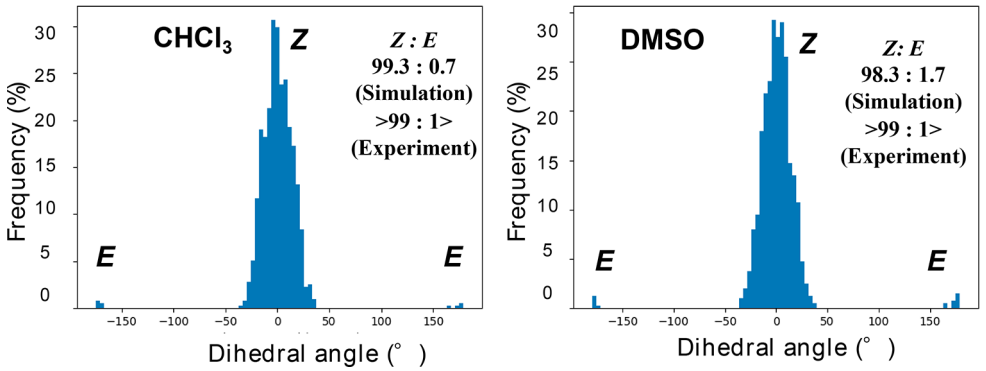

Figure 5. Distribution of Z/E isomers of NMe-thioamide **3b** obtained by REST simulations at 300 K in various solvents. Horizontal axis is the dihedral angle of the thioamide rotation: conformers between −50° and +50° are regarded as the Z conformer and conformers between −150° to −180° and 150° to 180° are regarded as the E conformer. The vertical axis is the frequency of the conformer (%).

conjugation will be enhanced (see Bond Model Analysis below).

4. Computational Study Based on Molecular Dynamics. In order to understand the roles of solvents, acetyl alkyl substituents, and *N*-methylation, we carried out molecular dynamics (MD) calculations, including explicit solvent molecules. Based on the behaviors of solvents found in the MD simulations, we carried out DFT calculations that included one or two explict solvent molecules in an implicit solvent model, which can mimic the more realistic solvation environment found in the MD calculations. These calculations revealed hydrogen bonding mainly between the thioamide NH proton and the solvent heteroatom(s) in polar solvents, and also identified a weak interaction of halogenated solvents ($CHCl_3$ and CH_2Cl_2) with the thioamide (NH−CS) functionality.

Replica Exchange with Solute Tempering (REST) Simulations. To investigate the solvent dependence of thioamide isomerization, we performed accelerated molecular dynamics simulations of **3a (p-Me)** using the replica exchange with solute tempering (REST) method[18] with the OPSL3e force field in various solvent systems (Figure 4; details of simulation: see the Experimental Section). The OPSL3e force field is improved by additional parametrization and becomes applicable to many organic compounds.[19] The Z/E ratio of NH-thioamide **3a** was simulated in various solvents at 966 K. The populations of Z and E conformations were calculated by using 1,000 snapshot structures in the trajectories at 300 K, obtained in the REST calculations in a different solvent, over the range of 300 to 966 K. In $CHCl_3$, the Z/E ratio was simulated to be 40:60 [experiment: 49:51] at 300 K. In the case of DMSO, the Z/E ratio was simulated to be 4:96 [experiment: 8:92]. Other solvent systems gave the following simulated values: CH_2Cl_2: 35:65 [experiment: 36:64] (Z/E); acetone: 12:88 [experiment: 11:89] (Z/E); methanol: 12:88 [experiment: 9:91] (Z/E). Therefore, the REST calculations are in good agreement with the experimental trend in the Z/E ratio of the thioamide **3a**.

The reduction of the Z isomer ratio in polar solvent from that in nonpolar solvent was also reproduced in the REST calculations for another NH-thioamides **1a (p-H)**: in $CHCl_3$: simulated value (Z/E): 37:63; experiment: 45:55; in CH_2Cl_2: simulated value (Z/E): 25:75; experiment: 33:67; in acetone: simulated value(Z/E): 21:79; experiment: 9:91; in methanol: simulated value (Z/E): 14:86; experiment: 9:91; in DMSO: simulated value(Z/E): 8:92; experiment: 8:92. Therefore, the MD based simulations clearly reproduce the experimental solvent effects on the Z/E ratio of the NH-thioacetamide.

On the other hand, similar REST simulations reproduced the lack of a significant solvent effect on the Z/E ratio in the case of the N-Me-thioacetamide, as well as the Z biases (Figure 5). The calculations reproduced the experimental bias of Z/E distribution of the N-Me thioamide **3b**: in $CHCl_3$: simulated value (Z/E): 99.3:0.7; experiment: >99:<1; in DMSO: simulated value(Z/E): 98.3:1.7; experiment: > 99:<1.

Radial Distribution Function (g(r)). The interactions between the thioamides and the solvent can be analyzed from the trajectories of MD simulations obtained at 300 K for 40 ns (force field: OPSL3e) by means of the radial distribution function ($g(r)$) (Figures 6 and 7),[20] which expresses the probability distribution of the distance between the two molecules in solution. The target atom in one molecule is placed at the origin, and the density of the target atom in the other molecule at the distance r is divided by the density of the bulk system. The horizontal axis is the distance between the atoms (Å), the left vertical axis is the radial distribution function $g(r)$ (blue line) with the ratio of the bulk solvent with solvent structure set to 1.0, and the right vertical axis (Figures 6 and 7) is the integrated number of solvents (red curve, coordination number), indicating how many molecules are found in the range of each coordination sphere.

1. Polar and Hydrogen-Bond-Donating Solvents Such as DMSO, Acetone, and MeOH. In polar and hydrogen-bond-donating solvents such DMSO, acetone, and protic MeOH, the oxygen atom of the solvent molecule can coordinate to the acidic NH proton of the NH-thioamide **3a**,[21] giving a distribution starting at 1.8 Å with a peak at approximately 2.1 Å for both Z and E thioamides (**(3a)NH---O(DMSO** or **acetone** or **CH_3OH)** in Figure 6a−c). From the volume integration of $g(r)$ in the range of 1.8−3.5 Å, approximately one molecule of the solvent interacts with the thioamide NH atom. The values of the radial distribution function ($g(r)$) and the coordination number of solvents at the first peak are smaller in the case of Z thioamide than those in the E thioamide (Figure 6). This is probably due to steric hindrance around the NH group of the Z thioamide conformer, such as the sulfur atom of the thioamide, which hampers access of solvent molecules to the NH moiety. This difference in solvent coordination between Z and E thioamide conformers may be attributed at least in part to the solvent dependency of the stability of these conformers: these three solvents, DMSO,

https://doi.org/10.1021/acs.joc.1c00801
J. Org. Chem. XXXX, XXX, XXX−XXX

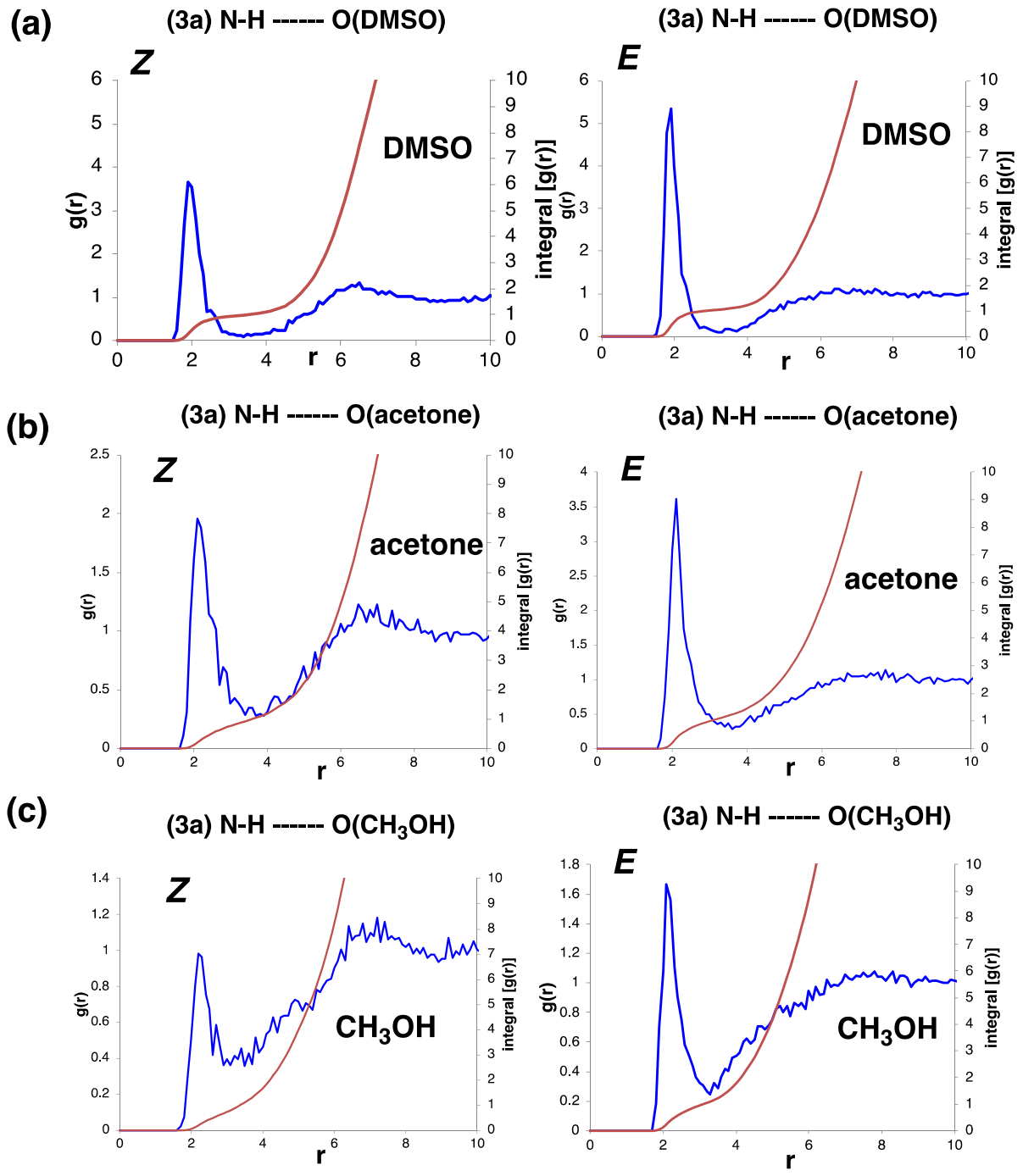

Figure 6. Radial distribution functions ($g(r)$) of NH-thioamide **3a** in polar solvents. Horizontal axis is the distance between the atoms (Å). The left vertical axis is the radial distribution function $g(r)$ (blue line): the ratio of the bulk solvent with solvent intrinsic structure is set to 1.0, and the right vertical axis is the integrated number of solvents (red curve, coordination number).

acetone and MeOH, favor NH-*E*-thioamide conformation (Table 2).

Furthermore, N-Me thioamides cannot form N−H (thioamide)---O (solvent) hydrogen bonding, as seen in NH-thioamide (**3a (p-Me)**). The RDFs of the solvent with respect to N-Me *Z*-thioacetamide (**3b (p-Me)**)) were obtained from the MD calculations and were compared with those of NH-thioamide (**3a (p-Me)**): in polar solvents, the RDFs of solvents around the N atom of the thioamide **3b** show no peaks at 2.1 Å (Figures S11b,c), and no significant association of solvent molecules around the N-Me moiety was observed (Figures S11d,e). Even in the case of protic methanol, methanol molecules show only weak hydrogen bonding at 2.7 Å through the interaction of the sulfur atom of N-Me *Z*-thioacetamide **3b** with the H-(OMe) atom of methanol (Figure S11b).

2. Halogenated Solvents Such as $CHCl_3$ and CH_2Cl_2. Although halogenated solvents such as $CHCl_3$ and CH_2Cl_2 can be regarded as nonpolar, they might also interact with NH-thioamide (**3a**) through hydrogen bonding between the acidic NH hydrogen atom of the thioamide and the chlorine atom(s) of the solvent ($CHCl_3$ and CH_2Cl_2) (**(3a)NH---Cl($CHCl_3$)** or **(3a)NH---Cl(CH_2Cl_2)**), in a manner similar to that of the

https://doi.org/10.1021/acs.joc.1c00801
J. Org. Chem. XXXX, XXX, XXX−XXX

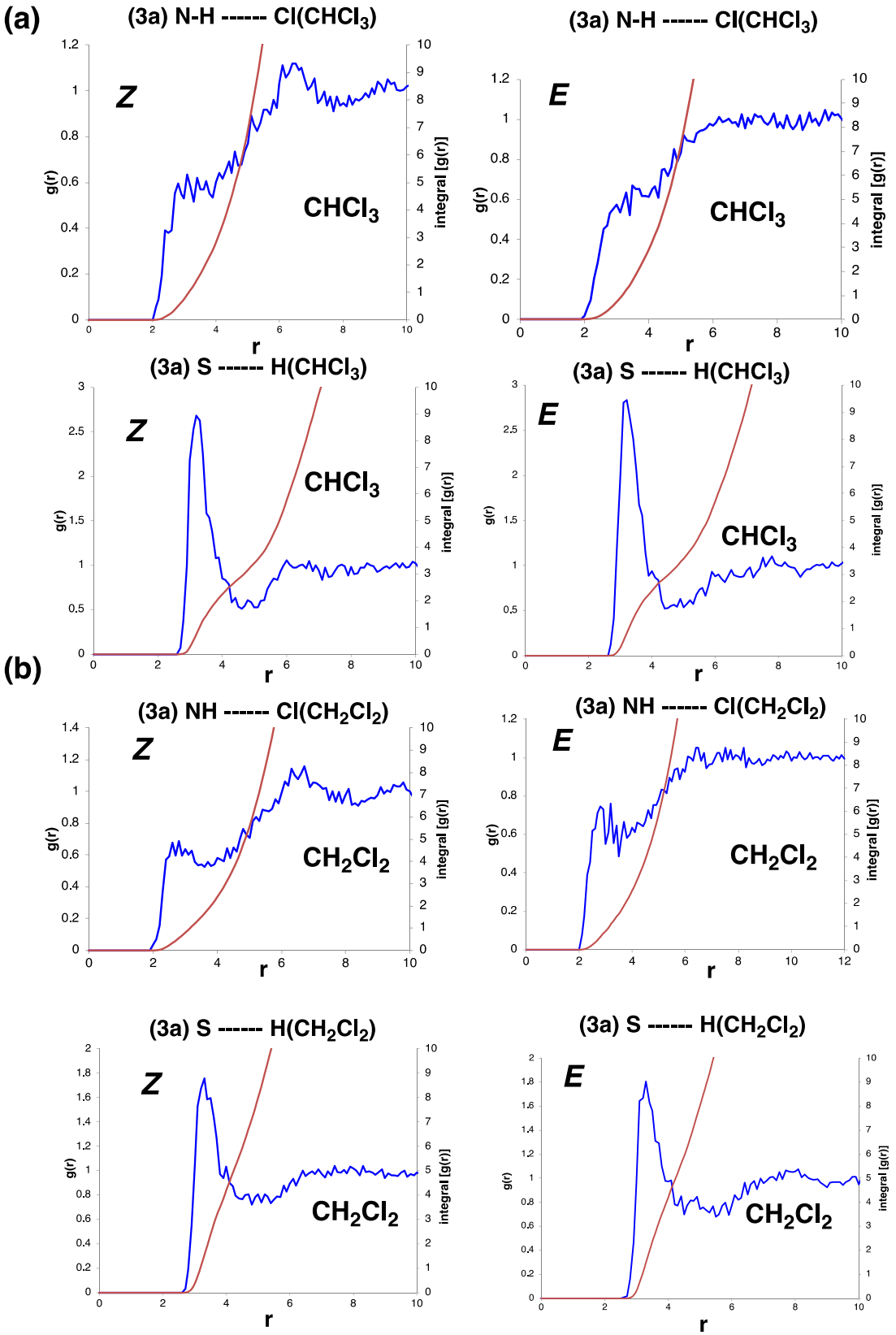

Figure 7. Radial distribution functions ($g(r)$) of NH-thioamide **3a** in halogenated solvent: (a) $CHCl_3$; (b) CH_2Cl_2. For details, see the caption of Figure 6.

aforementioned polar solvents. However, the radial distribution function analysis (Figure 7a,b) did not support the idea that such hydrogen bonding through H−Cl interaction of the NH-thioamide **3a** in CH_2Cl_2 or $CHCl_3$ is a significant contributor (Figure 7a,b):[20] there are multiple peaks from 2 to 4 Å in the radial distribution functions (Figure 7a,b), but the

https://doi.org/10.1021/acs.joc.1c00801
J. Org. Chem. XXXX, XXX, XXX−XXX

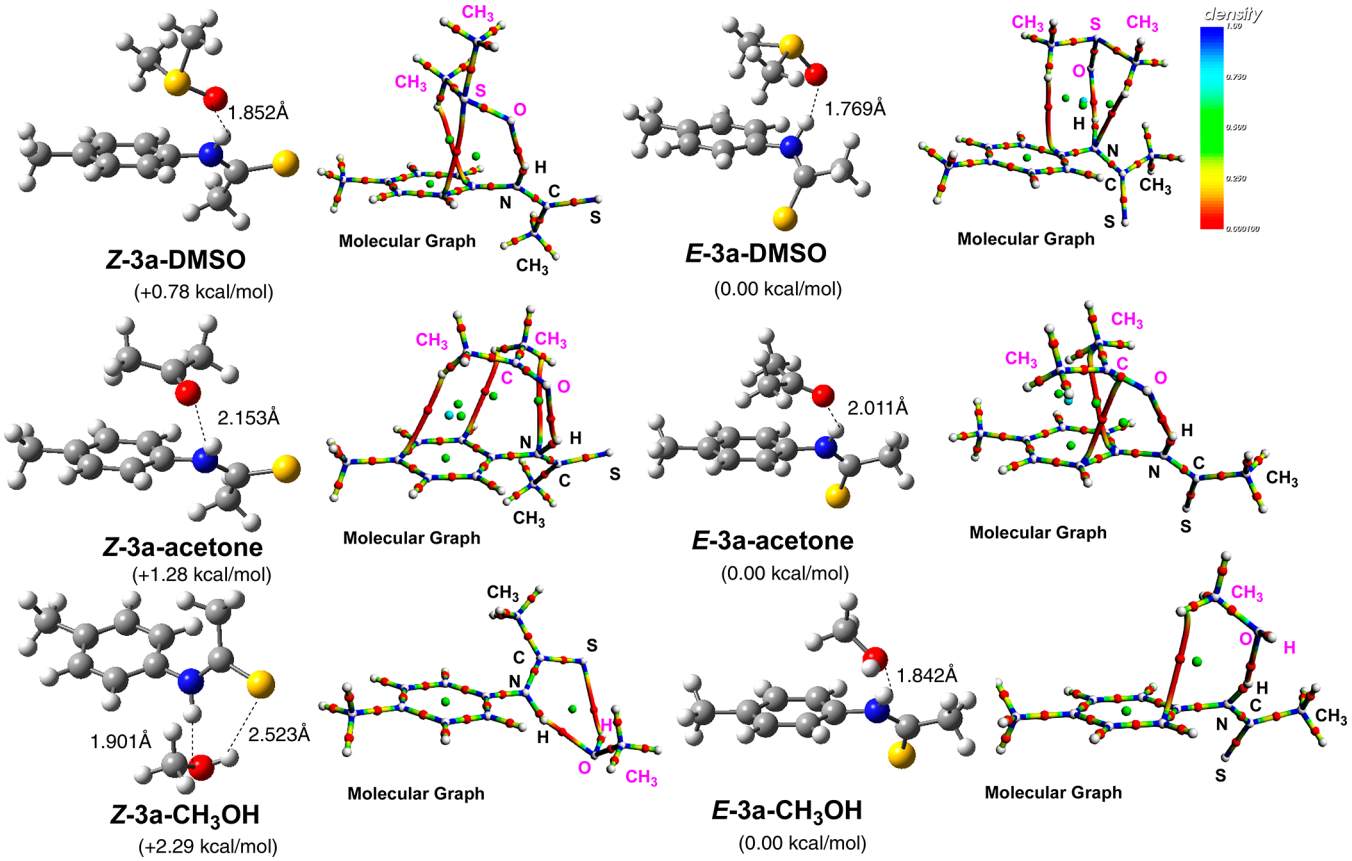

Figure 8. DFT-optimized structures of an arbitrary complex of a single polar solvent molecule and NH-thioamide **3a** and bond paths obtained by QTAIM calculations. In the ball-and-stick model, the dashed line indicates interaction, supported by the formation of a bond path in the QTAIM calculations. The colors have the following meaning: red: oxygen; blue: nitrogen; dark gray: carbon; white: hydrogen. In the molecular graph (QTAIM), the colors have the following meaning: a color-gradation line: accumulation of electron density (bond path for covalent bonding; red line: through-space weak bond path (with a purple arrow); red small ball: bond critical point, green small ball: ring critical point, blue small ball: cage critical point. Values in parentheses are the energy difference, based on the calculations with M062X/6-311++G(d) with the PCM solvent model, after zero-point energy correction and thermal correction to the energy at 300 K.

value of $g(r)$ is smaller than 1.0. Instead, hydrogen bonding between the sulfur atom of the thioamide and the solvent acidic hydrogen atom (H_2CCl_2 or $HCCl_3$), i.e., **(3a)S---H(CHCl$_3$)**) and CH_2Cl_2 (**(3a)S---H(CH$_2$Cl$_2$)**), contributes to the radial distribution function (Figure 7a,b). This putative hydrogen bonding is slightly more marked in the *Z* conformer than in the *E* conformer in terms of $g(r)$ value and coordination number at 4.0 Å. Intriguingly, integration of the $g(r)$ function in the range of 3.5−5 Å suggested there are multiple solvent molecules, perhaps five or six molecules, of $CHCl_3$ or CH_2Cl_2, around the S atom of the thioamide **3a**. Furthermore, in the case of N-Me *Z*-thioacetamide (**3b**) in $CHCl_3$, the **(3a)S---H(CHCl$_3$)**)-type interaction is maintained (Figure S11(a)).

DFT Calculations of Thioamide−solvent Complex. In order to gain more structural insight into solvent effects on the *Z*/*E* equilibrium of NH-*N*-phenylthioacetamides, we generated a solvent-coordinated thioamide model and conducted DFT calculations. The complex of thioamide **3a** hydrogen-bonded to a single molecule of solvent (also two molecules in the case of CH_2Cl_2) was selected as an arbitrary structure in the MD trajectory at 300 K, and the distance and angle of the solvent with respect to the thioamide were fully scanned. The resultant energy minimum candidate structure was fully optimized with M062X/6-311++G(d) in the PCM solvent model. We choose M062X because the standard B3LYP functional typically underestimates weak intermolecular interactions, which can be important for the solvent-stabilized complexes mentioned here.

The interaction of the solvent molecule with thioamide NH is visualized as a bond path (or a set of bond paths in a molecule (molecular graph); see the Experimental section), i.e., an accumulation of electron density between two atoms, obtained by means of Bader's quantum theory of atoms in molecules (QTAIM) calculations (Figure 8).[22] A similar hydrogen bond can be detected by QTAIM analysis in the cases of acetone and MeOH. Notably, in the case of a protic solvent, methanol, the *Z* conformation of thioamide **3a** forms two hydrogen bonds with one methanol molecule: there are hydrogen bonds between the thioamide NH and the oxygen atom of methanol and between the sulfur atom of the thioamide **3a** and the hydroxyl hydrogen atom of the same methanol molecule (Figure 8). In the case of halogenated solvents, the S(thioamide)−-H(solvent) bond path is present in $CHCl_3$ and CH_2Cl_2 (Figure S12), and this interaction is consistent with S−H(solvent) hydrogen bonding. In both $CHCl_3$ and CH_2Cl_2, the *Z* conformer can form two hydrogen bonds with the same halogenated solvent molecule, i.e., (thioamide)S−H(solvent) and (thioamide)NH---Cl(solvent) (Figure 9), which may contribution to stabilization of the *Z* conformation over the *E* conformation in $CHCl_3$ and CH_2Cl_2.

https://doi.org/10.1021/acs.joc.1c00801
J. Org. Chem. XXXX, XXX, XXX−XXX

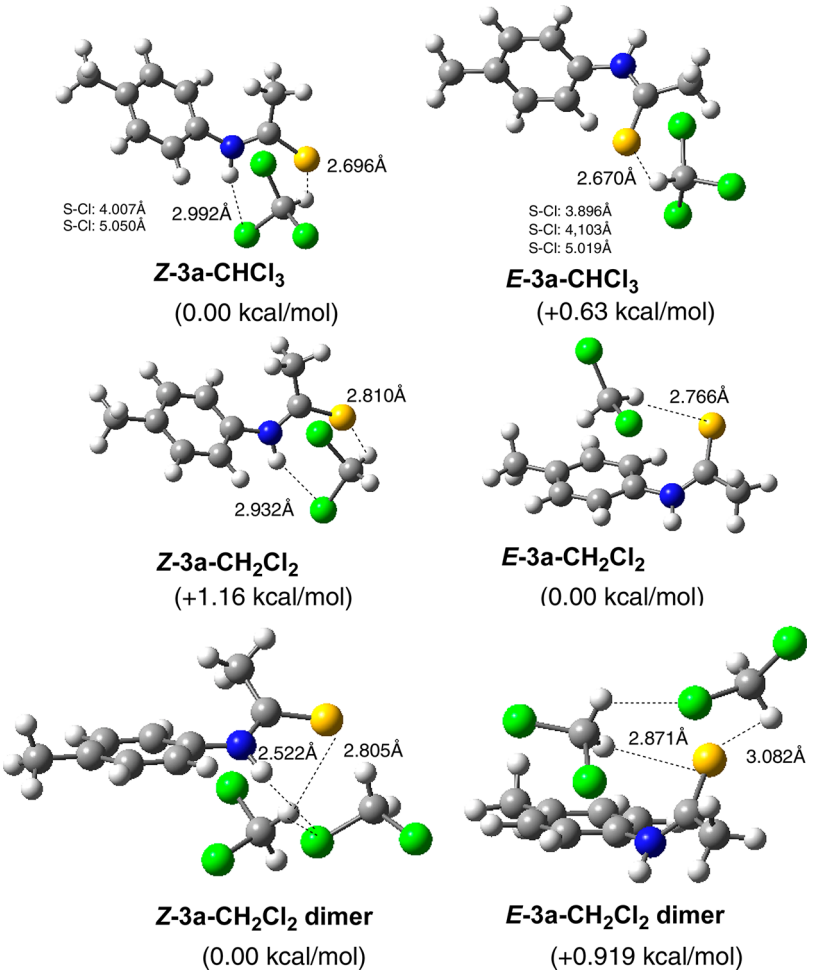

Figure 9. DFT-optimized structures of an arbitrary complex of one or two halogenated solvent molecules and NH-thioamide **3a**. For details, see the caption of Figure 8. Bond paths obtained in the QTAIM calculations; see Figure S13.

The energies of the *Z* and *E* structures complexed with a solvent molecule were calculated in polar solvents (Figure 8). In all of the polar solvents, the *E* isomer is more stable than the *Z* isomer (the energy differences are 0.78 kcal/mol (DMSO), 1.28 kcal/mol (acetone) and 2.29 kcal/mol (CH_3OH)) (M062X/6-311++G(d) with the PCM solvent model). These differences in stability correspond well to the shorter hydrogen bond length between the NH group of thioamide **3a** and the oxygen atom of the solvent in the *E* isomers. Therefore, polar solvents favor the *E* conformer over the *Z* conformer of the NH-thioamides **3a**.

On the other hand, in less polar halogenated solvents such $CHCl_3$ and CH_2Cl_2, S-hydrogen bonding may favor the *Z* conformation over the *E* conformation. In particular, as already mentioned, the *Z* conformer of thioamide (**3a**) can form two hydrogen bonds in $CHCl_3$ and in CH_2Cl_2. In $CHCl_3$, the *Z* form is more stable than the *E* form by 0.63 kcal/mol (Figure 9), while in CH_2Cl_2, the *E* conformer is more stable than the *Z* conformer by 1.16 kcal/mol (M062X/6-311++G(d) with the PCM solvent model). Because a cluster of halogenated solvent molecules surrounds the S atom of the thioamide, as indicated by the radial distribution function (Figure 7b, we made a minimal complex model of the thioamide with two molecules of CH_2Cl_2. The initial arbitrary structure was selected from a snapshot of the MD simulation at 300 K for 40 ns. Among several CH_2Cl_2 molecules, two CH_2Cl_2 molecules with a minimal distance between the S atom of the thioamide and H atom of CH_2Cl_2 were selected, followed by DFT structure optimization with the PCM solvent model. In this solvent dimer model, the *Z* form of the thioamide **3a** is more stable than the *E* form by 0.92 kcal/mol (Figure 9). The QTAIM molecular graph shows the presence of NH---Cl bonding and S−H (CH_2Cl_2) bonding, the interaction of two CH_2Cl_2 molecules, and also the double hydrogen bonding of the thioamide S atom with two H atoms of two CH_2Cl_2 molecules, together with the interaction of two CH_2Cl_2 molecules (Figure S13). The hydrogen bond distances are shorter in the *Z* conformer than the *E* conformer (Figure 9).

In halogenated solvents ($CHCl_3$ and CH_2Cl_2), hydrogen bonding between the thioamide sulfur atom and acidic H atom of the solvent favors *Z* conformation, probably due to enhancement of the thioamide resonance, while the *N*-phenyl π plane is twisted out of the thioamide π plane in the *Z* conformation. This *Z* preference of the thioamides is present but is not sufficiently strong to bias the equilibrium fully to *Z*, and a mixture of *Z* and *E* conformers is obtained.

The DFT calculations with only the implicit solvent model always resulted in the assessment that in the case of NH-thioacetamides the *E* isomer is more stable than the *Z* isomer in all the solvents studied herein (data not shown). Therefore, the present thioamide structures complexed with (a) solvent

https://doi.org/10.1021/acs.joc.1c00801
J. Org. Chem. XXXX, XXX, XXX−XXX

molecule(s) can mimic the more realistic solvation environment found in the MD calculations.

Bond Model Analysis. To elucidate the origin of the effect of *N*-methylation on *Z*/*E* thioamide preference (Table 2), we analyzed the electronic structures of the molecules in terms of the orbital interactions of thioacetamides (**1a**/**3a** and **1b**/**3b**) by means of bond model analysis (BMA) (Tables S2−S4).[23,24] The interbond energies (IBEs), including both occupied-occupied orbitals and occupied-vacant orbitals, were used to evaluate the bond interactions in the molecules. The IBEs were calculated for (1) vicinal bond interactions with respect to the thioamide N−C(S) bond, that is, between σ(C1−C2)/σ(C1−S) and σ(N−H)/σ(N−C(Ar)) (they are in a vicinal relation; see Figure 10), (2) conjugation between n(N) and C═S, n(N) and Ar, and C═S and Ar, and (3) repulsive interaction between two substituents attached to the thioamide bond, including all C−C and C−H σ bonds and π orbitals of the aromatic ring. Structures of NH-thioamides **1a** and **3a**, optimized with a single molecule of $CHCl_3$ solvent at M062X/6-311++G(d) in the SMD solvent mode (Figure 10), were used after elimination of the solvent molecule, and single point calculations at the level of HF/6-31G(d) were used for the bond orbital analysis. Structures of NMe-thioamides **1b** and **3b** were also optimized at the same level (M062X/6-311++G(d) in the SMD solvent mode) in $CHCl_3$, and single point calculations at the level of HF/6-31G(d) were used for the bond orbital analysis (Figure 12). The details are described in the Supporting Information.

(1) **1a**

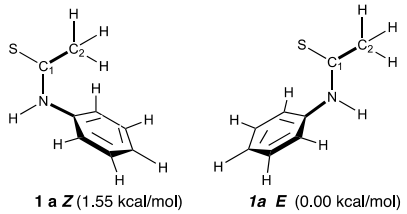

	1a-*Z*	**1a**-*E*	ΔIBE_{Z-E}
vicinal [a]	0.778	0.793	-0.015 [b]
conjugation [a]	-1.063	-1.080	0.016 [b]
repulsion [a]	0.736	0.500	0.236 [b]
total [c]	0.451 [c]	0.214 [c]	0.237 [d]

(2) **3a**

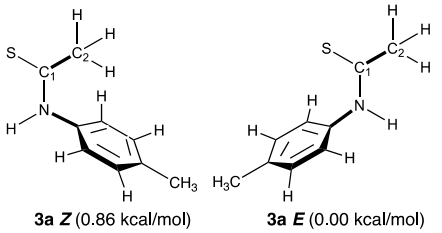

	3a-*Z*	**3a**-*E*	ΔIBE_{Z-E}
vicinal [a]	0.808	0.840	-0.032 [b]
conjugation [a]	-1.111	-0.911	-0.200 [b]
repulsion [a]	0.756	0.490	0.266 [b]
total [c]	0.454 [c]	0.419 [c]	0.035 [d]

Figure 10. Sum of interbond energies of NH-thioacetamides **1a** (1) and **3a** (2) in atomic units. (a) In au. For each term, a positive value indicates destabilization and a negative value indicates stabilization. For definitions of vicinal, conjugation, and repulsion, see the text. (b) The energy difference in interbond energies (IBE) (*Z* form − *E* form) is shown for each term. For each term, positive values indicate the *E* form is more stable, and negative values indicate the *Z* form is more stable. (c) "Total" is the sum of vicinal, conjugation, and repulsion terms for each conformer. (d) The energy difference in total interbond energies (IBE) (*Z* form − *E* form) is shown. A positive value indicates the *E* form is more stable, and a negative value indicates the *Z* form is more stable. In the graphics, the energy difference between the *Z* and *E* conformers, obtained at single-point calculation at HF/6-31G (d), is shown in parentheses.

In the case of NH-thioacetamides **1a**/**3a** (Figures 10), while the *Z*/*E* ratio varies depending on the solvent, the *E* isomer is more stable than the *Z* isomer. On the other hand, N-Me thioacetamides **1b**/**3b** exists solely as a *Z* rotamer (Figures 12). We analyzed the *Z* and *E* isomers of NH-thioacetamides **1a** and **3a** and those of the corresponding *N*-Me-thioacetamides **1b** and **3b**, respectively.

In the case of NH-thioacetamide **1a**, the total IBE is smaller in the *E* form by 0.237 au (ΔIBE_{Z-E} = +0.237 au) (Figure 10 (1)), showing an *E* preference. The sum of repulsive interactions is lower in the *E* form (0.500 au) than in the *Z* form (0.736 au), contributing to the *E* predominance (Figure 10 (1)). The repulsion energy between Me and Ph in the *Z* conformation is +0.356 au, whereas that of Me-H(N) in the E form is +0.162 au (see Table S2 (1) and Figure 11). Notably, the repulsion energy of n(S)-H(N) in the *Z* conformation (+0.380 au) is as large as that of n(S)-Ph (+0.389 au) in the *E* conformation (Table S2 (1) and Figure 11). NH-Thioacetamide **3a** (**p-Me**) shows similar trends (Figures 10 (2) and 11): the repulsion term is larger than the conjugation term in magnitude and sign and the repulsion in the *Z* conformation is significant: the repulsion IBE values are different between the *Z* and *E* conformers of **3a**: (Z-**3a**) Me-Ph: +0.365 au; (E-**3a**) Me-H(N): +0.161 au (Table S2 (2)). Thus, in the cases of NH-thioacetamides, the preference for *E* over *Z* conformation can be attributed to the repulsion effect in the *Z* conformation (Figure 11).

Furthermore, in the case of N-Me thioamide **1b** (Figures 12 (1)), the total IBE of the *Z* conformer (0.005 au) is smaller than that of the *E* conformer (0.251 au) by 0.246 au (ΔIBE_{Z-E} = −0.246), which is consistent with the experimentally observed *Z* preference. Among the vicinal, conjugation, and repulsion terms, the difference of conjugation interaction between *Z* and *E* (ΔIBE_{Z-E} = −0.332 au) is the main contributor to the total IBE difference for **1b** (Figures 12 (1)). In fact, the IBEs of the n(N)−π(C═S) conjugation are −2.120 au and −1.897 au in the *Z* and *E* conformations, respectively (Table S3 (1)), indicating significant stabilization of the *Z* conformer (Figure 12 (1)). The IBEs of n(N)-Ph conjugation are +0.414 au and +0.397 au in the *Z* and *E* conformers, respectively (Table S3 (1)), meaning that the n(N)-Ph conjugation interaction is repulsive, rather than stabilizing. Furthermore, the conjugation energy of C═(S) and Ph is +0.044 au in the *Z* conformer and +0.171 au in the *E* conformer, showing significant destabilization in the *E* conformation. This probably reflects a lower degree of conjugation between n(N) and π(Ph) in both of the *Z* and *E* structures, due to the lower degree of orbital overlap. With respect to the repulsion energy, the values of the sum of steric repulsion between two substituents that are syn along the thioamide bonds are similar in the *Z* and *E* conformations: Me-Ph (+0.414 au) and n(S)-Me (+0.457 au) in the *Z* conformer

https://doi.org/10.1021/acs.joc.1c00801
J. Org. Chem. XXXX, XXX, XXX−XXX

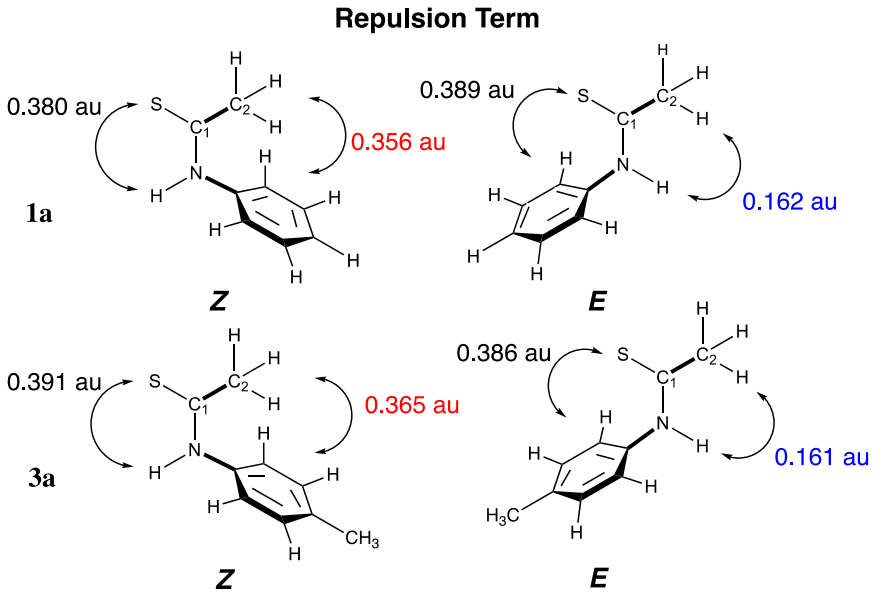

Figure 11. Summary of repulsive interactions in NH-thioamides **1a** and **3a** (see Supporting Information Table S2).

(1) **1b**

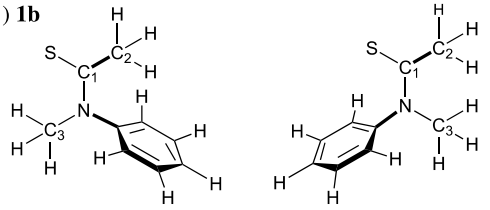

1b ***Z*** (0.00 kcal/mol) **1b** ***E*** (3.88 kcal/mol)

	1b-*Z*	**1b**-*E*	$\Delta IBE_{Z\text{-}E}$
vicinal [a]	0.795	0.769	0.026 [b]
conjugation [a]	-1.662	-1.329	-0.332 [b]
repulsion [a]	0.872	0.811	0.061 [b]
total [c]	0.005 [c]	0.251 [c]	-0.246 [d]

(2) **3b**

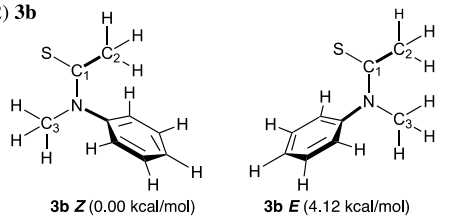

3b ***Z*** (0.00 kcal/mol) **3b** ***E*** (4.12 kcal/mol)

	3b-*Z*	**3b**-*E*	$\Delta IBE_{Z\text{-}E}$
vicinal [a]	0.821	0.792	0.029 [b]
conjugation [a]	-1.785	-1.303	-0.482 [b]
repulsion [a]	0.863	1.338	-0.475 [b]
Total [c]	-0.101	0.826	-0.927 [d]

Figure 12. Sum of interbond energies of *N*-methyl *N*-phenyl thioacetamides **1b** (1) and **3b** (2) in atomic units. (a−d) See the footnotes of Figure 11.

and Me-Me (+0.380 au) and *n*(S)-Ph (+0.429 au) in the *E* conformer (Table S3(1)).

NMe-Thioacetamide **3b** (**p-Me**) shows similar trends to **1b** (Figure 12 (2)): the difference in the conjugation term (−0.482 au) is larger than the vicinal interaction term (0.029 au) in magnitude and sign when we compare the *Z* and *E* conformers. Intriguingly, in the case of **3b**, the difference in the repulsion term (−0.475 au) between the *Z* and *E* conformers is also significant, both repulsion and conjugation terms favoring the *Z* conformer. The increase of the magnitude of the repulsion term (−0.475 au) arises from increased repulsion between Me(C1) and Me(N) (0.959 au) in the *E* conformation, probably due to the electron-donating nature of the aromatic *p*-methyl substituent (Table S3 (2)). Thus, in the cases of NMe-thioacetamides, the preference for *Z* over *E* conformation can be attributed to the conjugation effect in the *Z* conformation (Figure 12).

Based on the present orbital interaction analysis (BMA) and other calculations, we also consider that the solvent contributes to the *Z*/*E* isomer preference of NH-thioacetamides by means of hydrogen-bond formation between thioamide NH and the solvent molecule's heteroatom: hydrogen bonding of solvents to the NH proton of thioacetamides may increase steric repulsion with the sulfur atom in the *Z* conformation, making the *Z* thioamide conformation unfavorable in hydrogen-bond acceptor solvents. Thus, the equilibrium is biased to *E* preference, depending on the H-bond-forming ability of the solvent. Such a steric effect is absent in the case of *N*-methylated derivatives due to the intrinsically perpendicular arrangement of the N-benzene ring in the *Z* thioamide conformation. In the case of N-Me acetamide, steric repulsions have been attributed to cis predominance.[16] Therefore, counterintuitively, steric repulsion is the major factor influencing the *Z*/*E* preference of less sterically hindered NH-thioacetamides, while thioamide conjugation is the major factor influencing that of more sterically hindered *N*-methyl-thioacetamides.

Solvent Independency and Steric Effect in the *Z*/*E* Preference of Nonaromatic Thioacetamide 11a. As described above, the solvent dependency of the *Z*/*E* ratio of thioacetamides **1a**−**10a** can be attributed to hydrogen bonding of a solvent molecule to the NH proton of thioacetamides **1a**−**10a**, which partially enforces conjugation of the benzene ring of the aniline part (i.e., N-benzene) with the thioamide system in the *Z*/*E* conformations. In the *Z* conformers, this structural

https://doi.org/10.1021/acs.joc.1c00801
J. Org. Chem. XXXX, XXX, XXX−XXX

change results in increased steric repulsion. Therefore, the solvent effect on the *Z*/*E* isomers of thioacetamides appears to depend on the presence of the N-benzene moiety, which is affected by solvent NH-hydrogen bonding. To test this idea, we replaced the N-benzene ring with an *N*-methyl group, obtaining the nonaromatic thioacetamide **11a**. As expected, experimental examination showed that the solvent effect on the *Z*/*E* preference of NH-thioacetamide **11a** was greatly decreased (Table 2).

We also conducted REST simulations of **11a** in explicit solvent of $CHCl_3$, CH_2Cl_2, acetone, methanol, and DMSO (OPSL3e, 20 ns). The simulation also showed that the *E* isomer is favored over the *Z* isomer, accounting for more than 99% at 300 K (Figure S12), which accords well with the experimentally observed *E* preference (Table 2). Furthermore, bond model analysis showed that this nonaromatic NH-thioamide favors the *E* conformer due to strong repulsion between the two syn vicinal substituents in the *Z* isomer (the IBE difference in repulsion in total is 0.192 au): Me(C1)-Me3 (repulsion IBE: 0.296 au); *n*(S)-H(N) (repulsion IBE: 0.274 au) (Figure 13 and Table S4).

11a

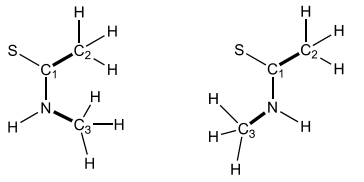

11a *Z* (2.19 kcal/mol) **11a *E*** (0.00 kcal/mol)

	11a-*Z*	11a-*E*	$\Delta IBE_{Z\text{-}E}$(11a)
vicinal [a]	0.601	0.625	-0.024 [b]
conjugation [a]	-1.389	-1.420	0.031 [b]
repulsion [a]	0.485	0.293	0.192 [b]
total [c]	-0.303	-0.502	0.199 [d]

Figure 13. Sum of interbond energies of nonaromatic **11a** in atomic units. (a−d) See the footnotes of Figure 11.

Therefore, the *E* thioamide preference of NH-thioacetamide **11a** is consistent with a key role of steric repulsion, as in the case of aromatic NH-thioacetamides.

CONCLUSION

We found that the *Z*/*E* isomer preference of NH-*N*-phenylthioacetamides shows significant solvent dependence due to hydrogen (H)-bond formation between thioamide NH and a solvent molecule: this hydrogen bonding forces the benzene ring of the aniline moiety (N-benzene) to adopt a coplanar arrangement with respect to the thioamide plane in the *Z* thioamide conformation, resulting in increased steric repulsion. Thus, the equilibrium is biased to the *E* conformer to an extent that depends on the H-bond-forming ability of the solvent. This steric effect is absent in the case of *N*-methylated derivatives due to the intrinsically perpendicular arrangement of the N-benzene ring in the *Z* thioamide conformation. This leads to the counterintuitive situation that the *Z*/*E* preference of NH-*N*-phenyl thioacetamides is determined by steric repulsion, while that of *N*-methyl-*N*-phenyl thioacetamides is determined by thioamide conjugation.

EXPERIMENTAL SECTION

General Procedure. Unless stated otherwise, commercial grade reagents were used without further purification. Open column chromatography was carried out using Kanto chemical silica gel (silica gel 60 N (100−210 μm)). One- and two-dimensional ^{1}H NMR (400 MHz) spectra and ^{13}C NMR (100 MHz) spectra were recorded on a Bruker Avance 400 NMR spectrometer running Topspin. The spectra were recorded at 20 °C, unless otherwise noted. ^{1}H NMR and ^{13}C NMR chemical shifts (δ) are given in parts per million (ppm) and coupling constants are given in hertz (Hz). s = singlet, brs = broad singlet, d = doublet, t = triplet, m = multiplet. ^{1}H NMR spectra are reported relative to residual solvent signals ($CDCl_3$: 7.26 ppm, DMSO-d_6: 2.50 ppm). Data for ^{13}C NMR spectra are reported in terms of chemical shift (ppm) relative to residual solvent peak ($CDCl_3$: 77.0 ppm, DMSO-d_6: 39.52 ppm). The ^{1}H NMR integrals of a mixture of thioamide rotamers are described as defining the methyl signal of the major rotamer as 3H. Electron spray ionization time-of-flight mass spectra (ESI-TOF MS) were recorded on a Bruker micrOTOF-05. The combustion analysis was carried out in the microanalytical laboratory of the University of Tokyo. All of the melting points were measured with a Yanaco Micro Melting Point Apparatus without correction.

Synthesis of Compounds. Thioanilides with various kinds of substituents (**1a−10a**, **1b−10b**) were synthesized by thionation of parent amides with Lawesson's reagent in toluene at 100 °C in oil bath.[25] First, theparent anilides were obtained by the reaction of acyl chloride (formyl chloride, acetyl chloride, propanoyl chloride, or cyclohexanoyl chloride) and para-substituted aniline in dimethylacetamide (DMAC) without addition of a base.[26] In the cases of *N*-methylanilides, para-substituted *N*-methylaniline was used. *N*-Methylation of *p*-methoxy *N*-phenylacetamide was performed with dimethyl sulfate in argon-bubbled DMSO in the presence of NaH, giving in 90% *N*-methylated amide.

Synthesis of Thioamides. *1a*.

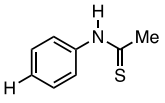

1a

Acetanilide (301.0 mg, 2.23 mmol) was dried *in vacuo* in a round-bottom flask for 2 h. Lawesson's reagent (540.5 mg, 1.34 mmol) and toluene (10 mL) were added into the flask, and the mixture was stirred at 100−110 °C in oil bath for 2 h under Ar atmosphere. The mixture was evaporated. The crude was column chromatographed (hexane/EtOAc = 6:1) to give **1a** (208.3 mg, 62%, colorless plates). Mp = 120−121 °C. ^{1}H NMR (400 MHz, $CDCl_3$) (mixture of rotamers) δ: 9.59 (0.8H, brs), 8.75 (1H, brs), 7.66 (2H, m), 7.45−7.33 (4.5H, m), 7.29−7.25 (1H, m), 7.17 (1.6H, d, J = 7.6 Hz), 2.74 (3H, s), 2.51 (3H, s). ^{13}C{^{1}H} NMR (100 MHz, $CDCl_3$) (mixture of rotamers) δ: 204.9, 200.6, 138.8, 138.1, 129.8, 129.1, 128.1, 127.1, 125.3, 124.0, 36.4, 30.1. HRMS (ESI-TOF) m/z: $[M + H]^+$ Calcd for $C_8H_{10}NS^+$, 152.0528, Found: 152.0535.

***2a*.**

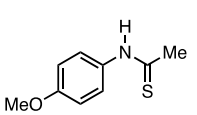

2a

p-Acetanisidide (151.5 mg, 0.92 mmol) was dried *in vacuo* in a round-bottom flask for 2 h. Lawesson's reagent (222.6 mg, 0.55 mmol) and toluene (10 mL) were added into the flask, and the mixture was stirred at 100−110 °C in oil bath for 2 h under Ar atmosphere. The mixture was evaporated. The crude was column chromatographed (hexane/EtOAc = 4:1) to give **2a** (101.0 mg, 61%), which was recrystallized by hexane and CH_2Cl_2 to afford colorless plates. Mp = 114−115 °C. ^{1}H NMR (400 MHz, $CDCl_3$) (a mixture of rotamers) δ: 9.46 (0.9H, brs), 8.70 (1H, brs), 7.50 (2H, d, J = 9.2 Hz), 7.09 (2H, d, J = 8.8 Hz), 6.93 (2H, d, J = 2.8 Hz), 6.90 (2H, d, J = 2.8 Hz), 3.82 (3H, s), 3.81 (3H, s), 2.72 (3H, s), 2.44 (3H, s). ^{13}C{^{1}H} NMR (100 MHz, $CDCl_3$) (a mixture of rotamers) δ: 205.2, 200.6, 159.3, 158.4, 131.8, 131.1, 126.9, 125.9, 114.9, 114.6, 55.7, 55.6, 35.9, 29.9.

https://doi.org/10.1021/acs.joc.1c00801
J. Org. Chem. XXXX, XXX, XXX−XXX

Anal. Calcd for $C_9H_{11}NOS$: C, 59.64; H, 6.12; N, 7.73. Found: C, 59.29; H, 6.08; N, 7.46. HRMS (ESI-TOF) m/z: $[M + Na]^+$ Calcd for $C_9H_{11}NOSNa^+$, 204.0454, Found: 204.0471.

3a.

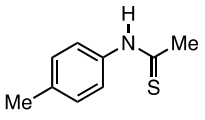

3a

N-(4-Chlorophenyl)acetamide (304.9 mg, 2.01 mmol) was dried *in vacuo* in a round-bottom flask for 2 h. Lawesson's reagent (488.8 mg, 1.21 mmol) and toluene (10 mL) were added into the flask, and the mixture was stirred at 100−110 °C in oil bath for 2 h under Ar atmosphere. The mixture was evaporated. The crude was column chromatographed (hexane/EtOAc = 6:1) to give **3a** (203.4 mg, 61%), which was recrystallized with hexane and EtOAc to afford colorless needles). Mp = 126−128 °C. ^{1}H NMR (400 MHz, $CDCl_3$) (mixture of rotamers) δ: 9.54 (0.9H, brs), 8.73 (1H, brs), 7.50 (2H, d, J = 8.4 Hz), 7.22−7.18 (4H, m), 7.04 (2H, d, J = 8.4 Hz), 2.72 (3H, s), 2.48 (3H, s), 2.37 (3H, s), 2.34 (3H, s). $^{13}C\{^1H\}$ NMR (100 MHz, $CDCl_3$) (mixture of rotamers) δ: 204.7, 200.5, 138.2, 137.1, 136.2, 135.6, 130.2, 129.6, 125.1, 124.1, 36.0, 30.0, 21.2, 21.1. Anal. Calcd for $C_9H_{11}NS$: C, 65.41; H, 6.71; N, 8.48. Found: C, 65.23; H, 6.75; N, 8.48. HRMS (ESI-TOF) m/z: $[M + Na]^+$ Calcd for $C_9H_{11}NNaS^+$, 188.0504, Found: 188.0531.

4a.

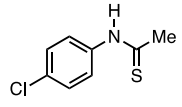

4a

N-(4-Chlorophenyl)acetamide (101.3 mg, 0.60 mmol) was dried *in vacuo* in a round-bottom flask for 2 h. Lawesson's reagent (146.2 mg, 0.36 mmol) and toluene (5 mL) were added into the flask, and the mixture was stirred in 100−110 °C in oil bath oil bath for 2 h under Ar atmosphere. The temperature was then changed to 90 °C and 3 drops water was added into the mixture and stirred for another 30 min. The mixture was dissolved in EtOAc, washed with saturated aqueous solution of $NaHCO_3$ and evaporated. The crude was column chromatographed (hexane/EtOAc = 8:1) to give **4a** (84.6 mg, 76%, white solid). Mp = 139−140 °C. ^{1}H NMR (400 MHz, $CDCl_3$) (mixture of rotamers) δ: 9.52 (0.4H, brs), 8.71 (1H, brs), 7.62 (2H, d, J = 8.8 Hz), 7.42−7.38 (1 H, m), 7.37−7.34 (2H, m), 7.11 (1H, d, J = 8.4 Hz), 2.73 (3H, s), 2.50 (1.4H, s). $^{13}C\{^1H\}$ NMR (100 MHz, $CDCl_3$) (mixture of rotamers) δ: 205.0, 200.9, 137.2, 136.6, 133.9, 132.3, 130.0, 129.2, 126.6, 125.3, 36.3, 30.2. Anal. Calcd for C_8H_8ClNS: C, 51.75; H, 4.34; N, 7.54. Found: C, 51.61; H, 4.48; N, 7.43. HRMS (ESI-TOF) m/z: $[M + H]^+$ Calcd for $C_8H_9ClNS^+$, 186.0139, Found: 186.0148.

5a.

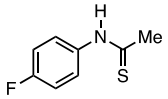

5a

4′-Fluoroacetanilide (304.9 mg, 1.99 mmol) was dried *in vacuo* in a round-bottom flask for 2 h. Lawesson's reagent (483.1 mg, 1.19 mmol) and toluene (6 mL) were added into the flask, and the mixture was stirred at 100−110 °C in oil bath for 2 h under Ar atmosphere. The mixture was evaporated. The crude was column chromatographed (hexane/EtOAc = 4:1) to give **5a** (113.8 mg, 34%, colorless plates). Mp = 80−81 °C. ^{1}H NMR (400 MHz, $CDCl_3$) (mixture of rotamers) δ: 9.36 (0.5H, brs), 8.63 (1H, brs), 7.62- 7.58 (2H, m), 7.18−7.07 (4H, m), 7.49−7.47 (0.1H, m), 2.74 (3H, s), 2.47 (1.7H, s). $^{13}C\{^1H\}$ NMR (100 MHz, DMSO-d_6) (mixture of rotamers) δ: 199.4, 159.5 (d, J = 241 Hz),135.9, 132.4, 127.2, 125.4, 115.9 (d, J = 23 Hz), 115.2 (d, J = 13 Hz), 115.0, 34.9, 30.7. Anal. Calcd for C_8H_8FNS: C, 56.19; H, 4.83; N, 8.19. Found: C, 56.26; H, 5.10; N, 7.89. HRMS (ESI-TOF) m/z: $[M + H]^+$ Calcd for $C_8H_9FNS^+$, 170.0434. Found: 170.0436.

6a.

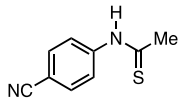

6a

4-Cyanoacetanilide (300.0 mg, 1.99 mmol) was dried *in vacuo* in a round-bottom flask for 2 h. The Lawesson's reagent (483.1 mg, 1.19 mmol) and toluene (6 mL) were added into the flask, and the mixture was stirred at 100−110 °C in oil bath for 2 h under Ar atmosphere. The mixture was evaporated. The crude was purified by flash column chromatographed (hexane/EtOAc = 8:1) to give **6a** (178.3 mg, 60%, yellow solid). Mp = 197−198 °C. ^{1}H NMR (400 MHz, DMSO-d_6) δ: 11.87 (1H, brs), 8.13 (2H, d, J = 6.8 Hz), 7.87 (2H, d, J = 6.8 Hz), 2.65 (3H, s). $^{13}C\{^1H\}$ NMR (100 MHz, DMSO-d_6) δ: 200.9, 143.5, 132.8, 122.7, 118.7, 107.6, 35.9. Anal. Calcd for $C_9H_8N_2S+ 0.1H_2O$: C, 60.72; H, 4.64; N, 15.73. Found: C, 60.58; H, 4.68; N, 15.55. HRMS (ESI-TOF) m/z: $[M + H]^+$ Calcd for $C_9H_9N_2S^+$, 177.0481. Found: 170.0483.

7a.

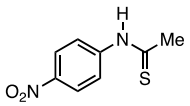

7a

p-Nitroacetanilide (300.4 mg, 1.67 mmol) was dried *in vacuo* in a round-bottom flask for 2 h. Lawesson's reagent (404.7 mg, 1.00 mmol) and toluene (10 mL) were added into the flask. and the mixture was stirred at 100−110 °C in oil bath for 2 h under Ar atmosphere. The mixture was evaporated. The crude was column chromatographed (hexane/EtOAc = 10:1 to 4:1) to afford **7a** (246.5 mg, 75%, yellow powder). Mp = 173−174 °C. ^{1}H NMR (400 MHz, DMSO-d_6) δ: 12.00 (1H, brs), 8.28 (2H, d, J = 9.2 Hz), 8.22 (2H, d, J = 9.2 Hz), 2.66 (3H, s). $^{13}C\{^1H\}$ NMR (100 MHz, DMSO-d_6) δ: 201.4, 145.2, 143.9, 124.3, 122.5, 36.0. Anal. Calcd for $C_8H_8O_2N_2S$: C, 48.98; H, 4.08; N, 14.28. Found: C, 48.97; H, 4.28; N, 14.15. HRMS (ESI-TOF) m/z: $[M + H]^+$ Calcd for $C_8H_9O_2N_2S^+$, 197.0379. Found: 197.0383.

8a.

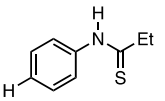

8a

N-Phenylpropionamide (100.7 mg, 0.74 mmol) was dried *in vacuo* in a round-bottom flask for 2 h. Lawesson's reagent (180.0 mg, 0.45 mmol) and toluene (5 mL) were added into the flask, and the mixture was stirred at 100−110 °C in oil bath for 260 min under Ar atmosphere. The mixture was evaporated. The crude was flash chromatographed (hexane/EtOAc = 8:1) to give **8a** (45.3 mg, 37%, yellow oil). ^{1}H NMR (400 MHz, $CDCl_3$) (mixture of rotamers) δ: 9.41 (1H, brs), 8.67 (1H, brs), 7.53 (2H, d, J = 7.6 Hz), 7.32−7.24 (3H,m), 7.15−7.11 (1H, m), 7.03 (0.6H, d, J = 7.2 Hz), 2.69 (2H, q, J = 7.6 Hz), 2.48 (0.7H, q, J = 7.6 Hz), 1.26 (3H, t, d, J = 7.6 Hz), 1.13 (1H, t, d, J = 7.4 Hz). $^{13}C\{^1H\}$ NMR (100 MHz, $CDCl_3$) (mixture of rotamers) δ: 138.7, 137,7, 129.7, 129.0, 128.1, 127.0, 125.6, 124.0, 41.7, 33.7, 13.9, 13.8. Anal. Calcd for $C_9H_{11}NS$: C, 65.41; H, 6.71; N, 8.48. Found: C, 65.30; H, 6.44; N, 8.15. HRMS (ESI-TOF) m/z: $[M + Na]^+$ Calcd for $C_9H_{11}NNaS^+$, 188.0504, Found: 188.0530.

9a.

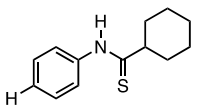

9a

N-Phenylcyclohexanecarboxamide (101.1 mg, 0.50 mmol) was dried *in vacuo* in a round-bottom flask for 2 h. Lawesson's reagent (120.7 mg, 0.30 mmol) and toluene (5 mL) were added into the flask, and the mixture was stirred at 100−110 °C in oil bath for 3 h under Ar atmosphere. The mixture was evaporated. The crude was column chromatographed (hexane/EtOAc = 2:1) to give **9a** (76.2 mg, 70%),

https://doi.org/10.1021/acs.joc.1c00801
J. Org. Chem. XXXX, XXX, XXX−XXX

which was recrystallized with hexane and $CHCl_3$ to afford coloreless needles). Mp = 132−133 °C. ^{1}H NMR (400 MHz, $CDCl_3$) (mixture of rotamers) δ: 9.20 (0.1H, brs), 8.58 (1H, brs), 7.67 (2H, d, J = 7.2 Hz), 7.46−7.42 (0.2H, m), 7.42−7.37 (2H, m), 7.28−7.24 (2H, m), 7.16 (0.3H, d, J = 7.6 Hz), 2.76- 2.71 (0.1H, m), 2.68−2.60 (1H, m), 2.03−2.00 (2H, m), 1.90−1.86 (2H, m), 1.84−1.57 (4H, m), 1.43−1.22 (3H, m), 1.13−1.06 (0.3H, m). ^{13}C{^{1}H} NMR (100 MHz, $CDCl_3$) (mixture of rotamers) δ: 210.0, 138.7, 129.8, 129.0, 128.2, 126.9, 125.7, 124.1, 56.7, 46.5, 33.5, 33.2, 26.1, 25.7, 25.7, 25.5. Anal. Calcd for $C_{13}H_{17}NS$+ 0.3H_2O: C, 69.47; H, 7.89; N, 6.23. Found: C, 69.79; H, 7.69; N, 6.30. HRMS (ESI-TOF) m/z: [M + H]$^+$ Calcd for $C_{13}H_{18}NS^+$, 220.1154, Found: 220.1156.

10a.

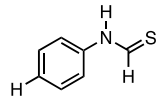

10a

THF (10 mL) was added into the mixture of formanilide (303.1 mg, 2.50 mmol) and Lawesson's reagent (607.4 mg, 1.50 mmol) at water bath (20 °C), and the solution was stirred at this temperature for 24 h. The mixture was evaporated. The crude was column chromatographed (hexane/EtOAc = 4:1) to give **10a** (123.7 mg, 36%, dark yellow oil). ^{1}H NMR (400 MHz, $CDCl_3$) δ: 9.77(1H, d, J= 14.8 Hz), 9.38 (1H, brs), 7.39−7.34 (2H, m), 7.24−7.20 (1H, m), 7.11 (2H, d, J = 7.2 Hz). ^{13}C{^{1}H} NMR (100 MHz, $CDCl_3$) δ: 187.4, 138.4, 130.0, 126.3, 117.4. Anal. Calcd for C_7H_7NS + 0.1H_2O: C, 60.49; H, 5.22; N, 10.08. Found: C, 60.63; H, 5.26; N, 9.74. HRMS (ESI-TOF) m/z: [M + H]$^+$ Calcd for $C_7H_8NS^+$, 138.0372, Found: 138.0369.

11a.

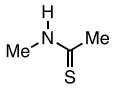

11a

N-Methylacetamide (306.1 mg, 4.2 mmol) was dried *in vacuo* in a round-bottom flask for 2 h. Lawesson's reagent (1953.5 mg, 4.83 mmol) and toluene (8 mL) were added into the flask, and the mixture was stirred at room temperature (25 °C) for 19 h under Ar atmosphere. The mixture was evaporated. The crude was column chromatographed (hexane/EtOAc = 7:3) to give **11a** (recrystallized by hexane and CH_2Cl_2 to afford 58.7 mg, 17%, white solid). Mp = 52−53 °C. ^{1}H NMR (400 MHz, $CDCl_3$) (a mixture of rotamers) δ: 7.38 (1H, brs), 3.17 (3H, d, J = 4.8 Hz), 3.02 (0.1H, d, J = 5.6 Hz), 2.56 (3H, t, J = 0.4 Hz), 2.50 (0.1H, s). ^{13}C{^{1}H} NMR (100 MHz, $CDCl_3$) δ: 201.8, 33.9, 33.2. Anal. Calcd for C_3H_7NS: C, 40.42; H, 7.91; N, 15.71. Found: C, 40.25; H, 7.74; N, 15.43. HRMS (ESI-TOF) m/z: [M + Na]$^+$ Calcd for $C_3H_7NNaS^+$, 112.0191, Found: 112.0193.

12a.

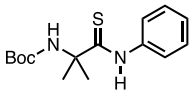

12a

tert-Butyl (2-methyl-1-oxo-1-(phenylamino)propan-2-yl)carbamate (301.2 mg, 1.09 mmol) was dried *in vacuo* in a round-bottom flask for 2 h. Lawesson's reagent (262.59 mg, 0.65 mmol) and toluene (8 mL) were added into the flask, and the mixture was stirred at 100−110 °C in oil bath for 2 h under Ar atmosphere. The mixture was evaporated. The crude was column chromatographed (hexane/EtOAc = 4:1) to give **12a** (114.6 mg, 36%, pale yellow powder). Mp = 116−117 °C. ^{1}H NMR (400 MHz, $CDCl_3$) δ: 10.41 (1H, brs), 7.68 (2H, d, J = 7.2 Hz), 7.44−7.37 (2H, m), 7.27−7.23 (1H, m), 1.74 (6H, s), 1.46 (9H, s). ^{13}C{^{1}H} NMR (100 MHz, $CDCl_3$) δ: 206.3, 155.6, 139.3, 129.0, 126.8, 123.8, 63.2, 29.1, 28.4. Anal. Calcd for $C_{15}H_{22}N_2O_2S$: C, 60.82; H, 7.55; N, 9.46. Found: C, 60.80; H, 7.40; N, 9.42. HRMS (ESI-TOF) m/z: [M + Na]$^+$ Calcd for $C_{15}H_{22}N_2O_2SNa^+$, 317.1294, Found: 317.1297.

1b.

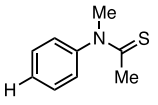

1b

N-Methylacetanilide (300.9 mg, 2.02 mmol) was dried *in vacuo* in a round-bottom flask for 2 h. Lawesson's reagent (489.5 mg, 1.21 mmol) and toluene (10 mL) were added into the flask, and the mixture was stirred at 100−110 °C in oil bath for 2 h under Ar atmosphere. The mixture was evaporated. The crude was column chromatographed (hexane/EtOAc = 4:1) to give **1b** (272.9 mg, 82%, coloreless plates). Mp = 49−50 °C. ^{1}H NMR (400 MHz, $CDCl_3$) δ: 7.48−7.44 (2H, m), 7.41−7.37 (1H, m), 7.18 (2H, d, J = 7.2 Hz), 3.74 (3H, s), 2.40 (3H, s). ^{13}C{^{1}H} NMR (100 MHz, $CDCl_3$) δ: 201.3, 145.9, 130.0, 128.5, 125.4, 45.8, 33.9. Anal. Calcd for $C_9H_{11}NS$: C, 65.41; H, 6.71; N, 8.48. Found: C, 65.40; H, 6.75; N, 8.43. HRMS (ESI-TOF) m/z: [M + H]$^+$ Calcd for $C_9H_{12}NS^+$, 166.0685, Found: 166.0690.

2b.

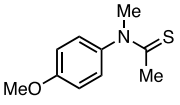

2b

N-(4-Methoxyphenyl)-*N*-methylacetamide ((204.4 mg, 1.14 mmol) was dried *in vacuo* in a round-bottom flask for 2 h. Lawesson's reagent (278.3 mg, 0.68 mmol) and toluene (5 mL) were added into the flask, and the mixture was stirred at 100−110 °C in oil bath for 2 h under Ar atmosphere. The mixture was evaporated. The crude was column chromatographed (hexane/EtOAc = 6:1) to give **2b** (189.3 mg, 85%, yellow oil). ^{1}H NMR (400 MHz, $CDCl_3$) δ: 7.09 (2H, d, J = 8.8 Hz), 6.94 (2H, d, J = 9.2 Hz), 3.84 (3H, s), 3.72 (3H, s), 2.39 (3H, s). ^{13}C{^{1}H} NMR (100 MHz, $CDCl_3$) δ: 201.7, 159.23, 138.8, 126.3, 115.0, 55.6, 45.9, 33.8. Anal. Calcd for $C_{10}H_{13}NOS$: C, 61.51; H, 6.71; N, 7.17. Found: C, 61.73; H, 6.70; N, 7.17. HRMS (ESI-TOF) m/z: [M + H]$^+$ Calcd for $C_{10}H_{14}NOS^+$, 180.0841, Found, 180.0839.

3b.

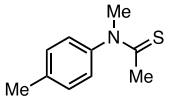

3b

N-Methyl-*N*-(*p*-tolyl)acetamide (175.8 mg, 1.08 mmol) was dried *in vacuo* in a round-bottom flask for 2 h. Lawesson's reagent (261.4 mg, 0.65 mmol) and toluene (3 mL) were added into the flask, and the mixture was stirred at 80 °C in oil bath for 24 h under Ar atmosphere. The mixture was evaporated. The crude was column chromatographed (hexane/EtOAc = 6:1) to give **3b** (175.4 mg, 98%, yellow oil). ^{1}H NMR (400 MHz, $CDCl_3$) δ: 7.25−7.22 (2H, m), 7.06−7.03 (2H, m), 3.72 (3H, d, J= 0.4 Hz), 2.39 (6H, t, J= 1.2 Hz). ^{13}C{^{1}H} NMR (100 MHz, $CDCl_3$) δ: 201.7, 143.7, 138.9, 130.9, 125.3, 46.1, 34.2, 21.4. Anal. Calcd for $C_{10}H_{13}NS$+ 0.1H_2O: C, 66.33; H, 7.35; N, 7.74. Found: C, 66.63; H, 7.07; N, 7.66. HRMS (ESI-TOF) m/z: [M + H]$^+$ Calcd for $C_{10}H_{14}NS^+$, 180.0841, Found, 180.0839.

4b.

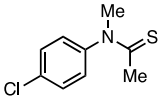

4b

N-(4-Chloro-phenyl)-*N*-methylacetamide (300.4 mg, 1.64 mmol) was dried *in vacuo* in a round-bottom flask for 2 h. Lawesson's reagent 396.94 mg, 0.98 mmol) and toluene (6 mL) were added into the flask, and the mixture was stirred at 100−110 °C in oil bath for 2 h under Ar atmosphere. The mixture was evaporated. The crude was column chromatographed (hexane/EtOAc = 2:1) to give **4b** (156.6 mg, 70.1%, white solid). Mp = 94−95 °C. ^{1}H NMR (400 MHz, $CDCl_3$) δ: 7.43 (2H, d, J = 8.8 Hz), 7.14 (2H, d, J = 8.8 Hz), 3.70 (3H, d, J = 0.4 Hz), 2.39 (3H, s). ^{13}C{^{1}H} NMR (100 MHz, $CDCl_3$) δ: 201.7, 144.3, 134.5, 130.3, 126.9, 45.7, 34.0. Anal. Calcd for $C_9H_{10}ClNS$: C, 54.13; H, 5.05; N, 7.01. Found: C, 53.94; H, 5.06; N, 6.96. HRMS (ESI-

https://doi.org/10.1021/acs.joc.1c00801
J. Org. Chem. XXXX, XXX, XXX−XXX

TOF) *m*/*z*: [M + H]$^+$ Calcd for $C_9H_{11}ClNS^+$, 200.0295, Found, 200.0316.

5b.

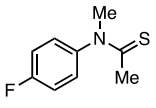

5b

4-Fluoro-*N*-methylaniline (120.1 mg, 0.72 mmol) was dried *in vacuo* in a round-bottom flask for 2 h. Lawesson's reagent 174.56 mg, 0.43 mmol) and toluene (5 mL) were added into the flask, and the mixture was stirred at 100−110 °C in oil bath for 4 h under Ar atmosphere. The mixture was evaporated. The crude was column chromatographed (hexane/EtOAc = 2:1) to give **5b** (101.6 mg, yellow oil, 77%). ^{1}H NMR (400 MHz, $CDCl_3$) δ: 7.19−7.12 (4H, m), 3.71 (3H, d, J = 0.4 Hz), 2.38 (3H, d, J = 0.4 Hz). $^{13}C\{^1H\}$ NMR (100 MHz, $CDCl_3$) δ: 201.7, 162.0 (J = 274 Hz), 142.0 (J = 3 Hz), 127.2 (J = 9 Hz), 117.0 (J = 22 Hz), 45.8, 33.9. Anal. Calcd for $C_9H_{10}FNS$: C, 58.99; H, 5.50; N, 7.64. Found: C, 58.86; H, 5.61; N, 7.64. HRMS (ESI-TOF) *m*/*z*: [M + H]$^+$ Calcd for $C_9H_{11}FNS^+$, 184.0591, Found, 184.0593.

6b.

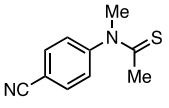

6b

N-(4-Cyanophenyl)-*N*-methylacetamide (150.1 mg, 0.89 mmol) was dried *in vacuo* in a round-bottom flask for 2 h. Lawesson's reagent 216.3 mg, 0.53 mmol) and toluene (6 mL) were added into the flask, and the mixture was stirred at 100−110 °C in oil bath for 14 h under Ar atmosphere. The mixture was evaporated. The crude was flash column chromatographed (hexane/EtOAc = 10:1) and open column chromatographed (hexane/EtOAc = 2:1) to give **6b** (37.6 mg, 22%, white solid). Mp = 112−113 °C. ^{1}H NMR (400 MHz, DMSO-d_6) δ: 8.00 (2H, d, J = 8.0 Hz), 7.66 (2H, d, J = 8.4 Hz), 3.63 (3H, brs), 2.30(3H, brs). $^{13}C\{^1H\}$ NMR (100 MHz, $CDCl_3$) δ: 201.6, 149.4, 134.1, 126.9, 117.7, 112.7, 45.6, 34.0. Anal. Calcd for $C_{10}H_{10}N_2S$+ $0.1H_2O$: C, 62.54; H, 5.35; N, 14.59. Found: C, 62.76; H, 5.49; N, 14.47. HRMS (ESI-TOF) *m*/*z*: [M + H]$^+$ $C_{10}H_{11}N_2S^+$, 191.0637, Found, 191.0640.

7b.

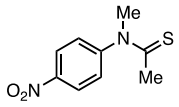

7b

N-Methyl-*N*-(4-nitrophenyl)acetamide (176.1 mg, 0.90 mmol) was dried *in vacuo* in a round-bottom flask for 2 h. Lawesson's reagent (219.0 mg, 0.54 mmol) and toluene (3 mL) were added into the flask, and the mixture was stirred at 100−110 °C in oil bath for 2 h under Ar atmosphere. The mixture was evaporated. The crude was column chromatographed (hexane/EtOAc = 4:1) to give **7a** (113.1 mg, 54%, yellow plates). Mp = 159−160 °C. ^{1}H NMR (400 MHz, $CDCl_3$) δ: 8.34 (2H, d, J= 8.8 Hz), 7.41 (2H, d, J= 8.8 Hz), 3.74 (3H, brs), 2.43 (3H, brs). $^{13}C\{^1H\}$ NMR (100 MHz, $CDCl_3$) δ: 201.7, 151.1, 147.3, 127.0, 125.6, 45.6, 34.1. Anal. Calcd for $C_9H_{10}O_2N_2S$: C, 51.41; H, 4.79; N, 13.32. Found: C, 51.41; H, 4.79; N, 13.32. HRMS (ESI-TOF) *m*/*z*: [M + H]$^+$ Calcd for $C_9H_{11}O_2N_2S^+$, 211.0536, Found: 211.0540.

8b.

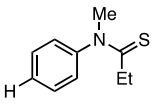

8b

N-methyl-*N*-phenylpropionamide (94.5 mg, 0.58 mmol) was dried *in vacuo* in a round-bottom flask for 2 h. Lawesson's reagent (140.5 mg, 0.35 mmol) and toluene (5 mL) were added into the flask, and the mixture was stirred at 100−110 °C in oil bath for 200 min under Ar atmosphere. The mixture was evaporated. The crude was column chromatographed (hexane/EtOAc = 2:1) to give **8b** (81.6 mg, 78%, yellow oil). ^{1}H NMR (400 MHz, $CDCl_3$) δ: 7.48−7.43 (2H, m), 7.41−7.37 (1H, m), 7.18−7.15 (2H, m), 3.72 (3H, s), 2.49 (2H, q, J= 7.2 Hz), 1.18 (3H, t, J= 7.2 Hz). $^{13}C\{^1H\}$ NMR (100 MHz, $CDCl_3$) δ: 207.8, 145.8, 130.1, 128.6, 125.6, 46.0, 37.2, 14.6. Anal. Calcd for $C_{10}H_{13}NS$+ $0.1H_2O$: C, 66.33; H, 7.35; N, 7.74. Found: C, 66.32; H, 7.15; N, 7.50. HRMS (ESI-TOF) *m*/*z*: [M + H]$^+$ Calcd for $C_{10}H_{14}NS^+$, 180.0845, Found: 180.0841.

9b.

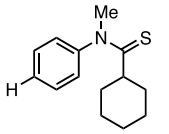

9b

N-Methyl-*N*-phenylcyclohexanecarboxamide (124.4 mg, 0.57 mmol) was dried *in vacuo* in a round-bottom flask for 2 h. Lawesson's reagent (138.9 mg, 0.34 mmol) and toluene (5 mL) were added into the flask, and the mixture was stirred at 100−110 °C in oil bath for 3 h under Ar atmosphere. The mixture was evaporated. The crude was column chromatographed (hexane/EtOAc = 2:1) to give **9b** (88.1 mg, 66%, white solid). Mp = 85−86 °C. ^{1}H NMR (400 MHz, $CDCl_3$) δ: 7.48−7.44 (2H, m), 7.43−7.38 (1H, m), 7.15−7.12 (2H, m), 3.70 (3H, s), 2.51−2.17 (1H, m), 1.84−1.74 (2H, m), 1.68−1.51 (5H, m), 1.21−1.14 (1H, m), 0.98−0.87 (2H, m). $^{13}C\{^1H\}$ NMR (100 MHz, $CDCl_3$) δ: 211.5, 145.9, 130.1, 128.5, 125.6, 49.5, 45.6, 33.7, 25.6, 25.5. Anal. Calcd for $C_{14}H_{19}NS$+ $0.2H_2O$: C, 70.96; H, 8.25; N, 5.91. Found: C, 70.93; H, 8.03; N, 5.79. HRMS (ESI-TOF) *m*/*z*: [M + H]$^+$ Calcd for $C_{14}H_{20}NS^+$, 234.1311, Found: 234.1327.

10b.

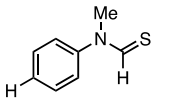

10b

THF (10 mL) was added into the mixture of formanilide (303.1 mg, 2.50 mmol) and Lawesson's reagent (607.4 mg, 1.50 mmol) in water bath (20 °C), and the solution was stirred at this temperature for 24 h. The mixture was evaporated. The crude was column chromatographed (hexane/EtOAc = 2:1) to give **10b** (123.7 mg, 36%, dark yellow oil). ^{1}H NMR (400 MHz, $CDCl_3$): 9.63(1H, d, J= 0.4 Hz), 7.45−7.41 (2H, m), 7.35−7.31 (1H, m), 7.26−7.21 (2H, m), 3.71 (3H, d, J= 0.4 Hz). $^{13}C\{^1H\}$ NMR (100 MHz, $CDCl_3$) δ: 189.3, 146.2, 129.9, 127.6, 122.0, 38.5. Anal. Calcd for C_8H_9NS + $0.2H_2O$: C, 62.06; H, 6.12; N, 9.05. Found: C, 62.16; H, 6.03; N, 9.09. HRMS (ESI-TOF) *m*/*z*: [M + H]$^+$ Calcd for $C_8H_{10}NS^+$, 152.0528, Found: 152.0524.

Synthesis of Amides. *1c*.

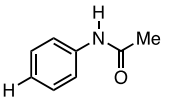

1c

A solution of acetyl chloride (790.5 mg, 10.07 mmol) in DMAC (5.0 mL) was made at room temperature and stirred at 0 °C for 5 min. A solution of aniline (935.2 mg, 10.04 mmol) in DMAC (5.0 mL) was added to the above solution slowly, and the mixture was stirred at 0 °C for another 5 min. The ice−water bath was removed, and the reaction went on for 170 min in water bath (20 °C). Water (30 mL) was added, and the mixture was stirred for 19 h. The mixture was extracted with ethyl acetate (20 mL) twice, and the organic fraction was washed with brine (40 mL). The organic layer was dried over Na_2SO_4 and filtered. The solvent was evaporated, and the residue was recrystallized with hexane and CH_2Cl_2 to afford **1c** (1023.5 mg, 76%, colorless plates). Mp = 105−108 °C. ^{1}H NMR (400 MHz, $CDCl_3$) δ: 7.89 (H, brs), 7.65 (2H, d, J = 7.6 Hz), 7.46 (2H, t, J = 7.8 Hz), 7.25 (1H, t, J = 7.4 Hz), 2.31 (3H, s). $^{13}C\{^1H\}$ NMR (100 MHz, $CDCl_3$) δ: 168.8, 138.0, 129.0, 124.4, 120.1, 24.6. Anal. Calcd for C_8H_9NO: C, 71.11; H, 6.67; N, 10.37. Found: C, 70.81; H, 6.79; N,10.32. HRMS (ESI-TOF) *m*/*z*: [M + H]$^+$ Calcd for $C_8H_{10}NO^+$, 136.0757, Found: 136.0766.

https://doi.org/10.1021/acs.joc.1c00801
J. Org. Chem. XXXX, XXX, XXX−XXX

2c.

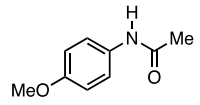

2c

A solution of acetyl chloride (789.8 mg, 10.12 mmol) in DMAC (5.0 mL) was made at room temperature and stirred at 0 °C for 5 min. A solution of *p*-anisidine (1232.1 mg, 10.00 mmol) in DMAC (5.0 mL) was added to the above solution slowly, and the mixture was stirred at 0 °C for another 5 min. The ice−water bath was removed and the reaction went on for 90 min in water bath (20 °C). Water (30 mL) was added, and the mixture was stirred for 18 h. The mixture was extracted with ethyl acetate (20 mL) twice, and the organic fraction was washed with brine (40 mL). The organic layer was dried over Na_2SO_4 and filtered. The solvent was evaporated and the residue was recrystallized with ethanol to afford **2c** (1152.5 mg, 70%, pink plates). Mp = 120−121 °C. ^{1}H NMR (400 MHz, $CDCl_3$) δ: 7.66 (1H, brs), 7.38 (2H, d, J = 9.2 Hz), 6.82 (2H, d, J= 8.8 Hz), 3.767 (3H, s), 2.120 (3H, s). $^{13}C\{^1H\}$ NMR (100 MHz, $CDCl_3$) δ: 168.7, 156.4, 131.1, 122.1, 114.0, 55.4, 24.2. Anal. Calcd for $C_9H_{11}NO_2$: C, 65.45; H, 6.67; N, 8.48. Found: C, 64.92; H, 6.64; N, 8.44. HRMS (ESI-TOF) m/z: $[M + H]^+$ Calcd for $C_9H_{12}NO_2^+$, 166.0863, Found: 166.0868.

3c.

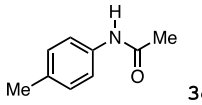

3c

A solution of acetyl chloride (782.0 mg, 10.04 mmol) in DMAC (5.0 mL) was made at room temperature and stirred at 0 °C for 5 min. A solution of *p*-toluidine (1072.8 mg, 10.01 mmol) in DMAC (5.0 mL) was added to the above solution slowly, and the mixture was stirred at 0 °C for another 5 min. The ice−water bath was removed, and the reaction went on for 70 min in water bath (16 °C). Water (30 mL) was added, the mixture was extracted with ethyl acetate (20 mL) twice, and the organic fraction was washed with brine (40 mL). The organic layer was dried over Na_2SO_4 and filtered. The solvent was evaporated, and the residue was recrystallized with hexane and EtOAc to afford **3c** (1118.3 mg, 79%, colorless plates). Mp = 78−79 °C. ^{1}H NMR (400 MHz, $CDCl_3$) δ: 7.44 (H, brs), 7.37 (2H, d, J = 8.4 Hz), 7.10 (2H, d, J= 8.0 Hz), 2.30 (3H, s), 2.14 (3H, s). $^{13}C\{^1H\}$ NMR (100 MHz, $CDCl_3$) δ: 168.4, 135.4, 134.0, 129.5, 120.1, 24.5, 20.9. Anal. Calcd for $C_9H_{11}NO$: C, 72.48; H, 7.38; N, 9.40. Found: C, 72.50; H, 7.38; N, 9.32. HRMS (ESI-TOF, [M + Na] $^+$): Calcd for $C_9H_{11}NONa^+$, 172.0733, Found: 172.0730.

Synthesis of *N*-(4-Methoxyphenyl)-*N*-methylacetamide.

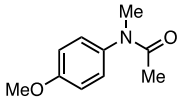

(intermediate of **2b**)

N-Methylation of *p*-methoxy-*N*-phenylacetamide was performed with dimethyl sulfate in argon-bubbled DMSO in the presence of NaH, giving in 90% *N*-methylated amide. To argon gas-bubbled DMSO (20 mL), NaH (60%, 562.7 mg, 1.4 equiv) was added by portions in a water−ice bath (15 °C) over 5 min. After 15 min, a solution of *p*-methoxy-*N*-phenylacetamide (1.6527g, 10 mmol) in 6 mL of argon gas-bubbled DMSO was added over 5 min at 15 °C. After the mixture was stirred for 80 min at 15 °C, 100 mL of water was added. The whole was extracted with dichloromethane (60 mL × 3), and the organic layer was washed with water and dried over $MgSO_4$. The organic solvent was evaporated to give a colorless viscous oil, which was open column-chromatographed (with ethyl acetate/*n*-hexane 3:2) to give the target *N*-methyl amide **2d** (1.6620g, 93% yield) as colorless plates. Mp = 54−55 °C. ^{1}H NMR (400 MHz, $CDCl_3$) δ: 7.08 (2H, d, J = 9.2 Hz), 6.90 (2H, d, J = 9.2 Hz), 3.81 (3H, s), 3.21 (3H, s), 1.83 (3H, s). $^{13}C\{^1H\}$ NMR (100 MHz, $CDCl_3$) δ: 170.9, 158.8, 137.4, 128.1, 114.8, 55.4, 37.2, 22.2. Anal. Calcd for $C_{10}H_{13}NO_2$: C, 67.02; H, 7.31; N, 7.82. Found: C, 66.99; H, 7.25; N, 7.70. HRMS (ESI-TOF) m/z: $[M + Na]^+$ Calcd for $C_{10}H_{13}NO_2Na^+$, 202.0838, Found, 202.0835.

X-ray Crystallographic Analysis. The details of X-ray crystallographic analyses of **3a**, **3c**, **5a**, and **7b** are given in Supporting Information.

Calculations of Solvation Model. To investigate the conformational preference and the distribution of conformations in solution, an accelerated molecular dynamics (MD) simulation, that is, replica exchange with solute tempering (REST) simulation,[18] was performed in the presence of explicit solvent molecules. Replica exchange with solute tempering (REST) simulation was performed with Desmond. The OPLS3e force field[19] was used for a thioamide and predefined model was used for each solvent. The custom solvent model box was created for chloroform. The systems initially contained solvents in orthorhombic boxes with at least 10.0 Å gap between the solute and the periodic boundaries. Using REST, we simulated thioamide isomerization with the OPLS3e force field in Desmond implemented in the Schrödinger software suite Maestro 2018−4. Simulations were performed for 40 ns using 8 replicas with an effective temperature of the solute from 300 K through about 965 K with NPT ensemble. The exchange rate was more than 30% for each simulation. The trajectory structures were saved every 4 ps (total 1000 frames) from the replica at 300 K. The conformations were classified into Z and E thioamides according to the following criteria: the horizontal axis is the dihedral angle of the thioamide rotation: conformers between −90° to +90° are regarded as *Z* and conformers between −180° to −90° and 90° to 180° are regarded as *E*. The vertical axis is the frequency (%) of the conformer.

Radial Distribution Function ($g(r)$). The interactions between the thioamides and the solvent can be analyzed for the trajectories of MD simulations obtained at 300 K for 40 ns (force field: OPSL3e) by use of the radial distribution function ($g(r)$),[20] which expresses the probability distribution of the distance between two molecules in a solution.

DFT Calculations of Thioamide and Solvent Complex. A complex of **3a** and a single molecule of the solvent (also two molecules in the case of CH_2Cl_2) hydrogen bonding to the thioamide **3a** was selected as an arbitrary structure in the MD trajectory at 300 K in the REST calculations, and the distance and angle of the solvent with respect to the thioamide were fully scanned. The resultant energy minimum candidate structure was fully optimized (default: SCF = tight) with M062X/6-311++G(d) in the IEFPCM solvent model with the Gaussian 16 program.[27] All the structures are energy minima in terms of the absence of negative frequency. Total energy of the molecules in the DFT calculations was subjected to zero-point corrections and thermal corrections without scaling, if not otherwise specified.

QTAIM Calculations. Bond-path analysis was performed at the Slater-type triple-ζ-polarization (TZP) level with ADF (SCM, Netherlands).[28] A polarization function is added for H through Ar and for Ga through Kr. Details of optimization of Slater-type basis sets were reported previously.[28] The QTAIM analysis was applied on the basis of the DFT-optimized energy-minimum structures.

What Is the Bond Path? The concepts of bond paths and bond critical points have been criticized and a rebuttal published.[22] There has also been controversy regarding the presence/absence of a bond path between unusual sets of atoms in different systems (see ref 17). A bond path is often misidentified with a chemical bond, but bond paths have been regarded as indicative of *bonded interactions*, not chemical bonds, and may encompass all kinds of interactions. Usually, covalent bonding corresponds well to the bond path. One of the different interpretations of a bond path involving *weak interactions* is that "simply allowing two atoms to approach each other should often cause electron density to flow to the interatomic space, depending on the balance between nucleus-electron attraction and electron-electron repulsion, both coulomb and exchange". QTAIM atoms are not simple spheres, and thus, their neighborhood can be influenced by their complex topology. This can lead to a bond path with a bond critical point, even in the purely classical case in which exchange is not considered. This analysis suggests that the occurrence of a bond critical point should depend on the interatomic distance (see ref 22e).

Bond Analysis of Thioamides. The electronic structures of the molecules were analyzed using bond model analysis,[23,24] which is able

https://doi.org/10.1021/acs.joc.1c00801
J. Org. Chem. XXXX, XXX, XXX−XXX

to evaluate the bond orbital interactions in molecules. The interbond energies (IBEs), including both occupied-occupied orbitals and occupied-vacant orbitals, were used to evaluate the bond interactions in the molecules. The IBEs were calculated for: (1) **vicinal interaction term (vicinal):** vicinal bond interactions with respect to the thioamide N−C(S) bond, that is, between σ(C1−C2)/σ(C1−S), and σ(N−H) or σ(N−C(Ar)) (they all are in a vicinal relation) (2) **conjugation interaction term (conjugation):** conjugation between n(N) and C═S, n(N) and Ar, and C═S and Ar, and (3) **repulsive interaction term (repulsion):** repulsive interaction between two substituents attached to the thioamide bond, including all C−C and C−H σ bonds and π orbitals of the aromatic ring.

■ ASSOCIATED CONTENT

Supporting Information

The Supporting Information is available free of charge at https://pubs.acs.org/doi/10.1021/acs.joc.1c00801.

NMR assignment of Z/E of thioamides (Figures S1−S3 and Table S1), X-ray crystallographic data (Figures S4−S10), calculation data (Figures S11−S13 and Tables S2−S4), calculation coordinates, and ^{1}H and ^{13}C{H} NMR spectral spectra (PDF)

Accession Codes

CCDC 2060674−2060677, 2072313−2072314, and 2075800 contain the supplementary crystallographic data for this paper. These data can be obtained free of charge via www.ccdc.cam.ac.uk/data_request/cif, or by emailing data_request@ccdc.cam.ac.uk, or by contacting The Cambridge Crystallographic Data Centre, 12 Union Road, Cambridge CB2 1EZ, UK; fax: +44 1223 336033.

■ AUTHOR INFORMATION

Corresponding Author

Tomohiko Ohwada − *Graduate School of Pharmaceutical Sciences, University of Tokyo, Bunkyo-ku, Tokyo 113-0033, Japan;* orcid.org/0000-0001-5390-0203; Email: ohwada@mol.f.u-tokyo.ac.jp

Authors

Shuyi Song − *Graduate School of Pharmaceutical Sciences, University of Tokyo, Bunkyo-ku, Tokyo 113-0033, Japan*

Tadashi Hyodo − *Faculty of Pharmaceutical Sciences at Kagawa Campus, Tokushima Bunri University, Sanuki, Kagawa 769-2193, Japan*

Hirotaka Ikeda − *Graduate School of Pharmaceutical Sciences, University of Tokyo, Bunkyo-ku, Tokyo 113-0033, Japan*

Kim Anh L. Vu − *Graduate School of Pharmaceutical Sciences, University of Tokyo, Bunkyo-ku, Tokyo 113-0033, Japan; NUS Graduate School for Integrative Sciences and Engineering, National University of Singapore, Singapore 119077; Cancer Science Institute of Singapore, National University of Singapore, Singapore 117599*

Yulan Tang − *Graduate School of Pharmaceutical Sciences, University of Tokyo, Bunkyo-ku, Tokyo 113-0033, Japan*

Erika S. Chan − *Graduate School of Pharmaceutical Sciences, University of Tokyo, Bunkyo-ku, Tokyo 113-0033, Japan; Ernest Mario School of Pharmacy, Rutgers, The State University of New Jersey, Piscataway, New Jersey 08854, United States*

Yuko Otani − *Graduate School of Pharmaceutical Sciences, University of Tokyo, Bunkyo-ku, Tokyo 113-0033, Japan;* orcid.org/0000-0002-8104-283X

Satoshi Inagaki − *Graduate School of Pharmaceutical Sciences, University of Tokyo, Bunkyo-ku, Tokyo 113-0033, Japan*

Kentaro Yamaguchi − *Faculty of Pharmaceutical Sciences at Kagawa Campus, Tokushima Bunri University, Sanuki, Kagawa 769-2193, Japan;* orcid.org/0000-0002-2629-716X

Complete contact information is available at: https://pubs.acs.org/10.1021/acs.joc.1c00801

Notes

The authors declare no competing financial interest.

■ ACKNOWLEDGMENTS

The computations were performed at the Research Center for Computational Science, Okazaki, Japan. This work was supported by Grants-in-Aid for Scientific Research (KAKENHI) (TO: 18H02552) provided by Japan Society for the Promotion of Science. K.A.L.V. is grateful to the Amgen Scholars Program for funding a study visit at the University of Tokyo.

■ REFERENCES

(1) (a) Jagodziński, T. S. Thioamides as Useful Synthons in the Synthesis of Heterocycles. *Chem. Rev.* **2003**, *103* (1), 197−228. (bc) Barrett, T. M.; Chen, X. S.; Liu, C.; Giannakoulias, S.; Phan, H. A. T.; Wang, J.; Keenan, E. K.; Karpowicz, R. J., Jr; Petersson, J. E. Studies of Thioamide Effects on Serine Protease Activity Enable Two-Site Stabilization of Cancer Imaging Peptides. *ACS Chem. Biol.* **2020**, *15*, 774−779. (d) Yang, J.; Wang, C.; Yao, C.; Chen, C.; Hu, Y.; He, G.; Zhao, J. Site-Specific Incorporation of Multiple Thioamide Substitutions into a Peptide Backbone via Solid Phase Peptide Synthesis. *J. Org. Chem.* **2020**, *85*, 1484−1494. (e) Maini, R.; Kimura, H.; Takatsuji, R.; Katoh, T.; Goto, Y.; Suga, H. Ribosomal Formation of Thioamide Bonds in Polypeptide Synthesis. *J. Am. Chem. Soc.* **2019**, *141*, 20004−20008. (f) Camacho, L. A., III; Nguyen, Y. H.; Turner, J.; VanVeller, D. Deprotection Strategies for Thioimidates during Fmoc Solid-Phase Peptide Synthesis: A Safe Route to Thioamides. *J. Org. Chem.* **2019**, *84*, 15309−15314. (h) Goldberg, J. M.; Batjargal, S.; Petersson, E. J. Thioamides as Fluorescence Quenching Probes: Minimalist Chromophores to Monitor Protein Dynamics. *J. Am. Chem. Soc.* **2010**, *132* (42), 14718−14720.

(2) (a) Gorske, B. C.; Nelson, R. C.; Bowden, Z. S.; Kufe, T. A.; Childs, A. M. Bridged n→π* interactions can stabilize peptoid helices. *J. Org. Chem.* **2013**, *78*, 11172−11183. (b) Laursen, J. S.; Engel-Andreasen, J.; Fristrup, P.; Harris, P.; Olsen, C. A. Cis−trans-amide bond rotamers in β-peptoids and peptoids: Evaluation of stereoelectronic effects in backbone and side chains. *J. Am. Chem. Soc.* **2013**, *135*, 2835−2844. (c) Camacho, L. A., III; Lampkin, B. J.; VanVeller, B. A Bottom-Up Approach To Preserve Thioamide Residue Stereochemistry during Fmoc Solid-Phase Peptide Synthesis. *Org. Lett.* **2019**, *21*, 7015−7018. (d) Dunbar, K. L.; Dell, M.; Molloy, E. M.; Kloss, F.; Hertweck, C. Reconstitution of Iterative Thioamidation in Closthioamide Biosynthesis Reveals Tailoring Strategy for Nonribosomal Peptide Backbones. *Angew. Chem., Int. Ed.* **2019**, *58*, 13014−13018. (e) Saito, M.; Murakami, S.; Nanjo, T.; Kobayashi, Y.; Takemoto, Y. Mild and Chemoselective Thioacylation of Amines Enabled by the Nucleophilic Activation of Elemental Sulfur. *J. Am. Chem. Soc.* **2020**, *142*, 8130−8135. (f) Newberry, R. W.; VanVeller, B.; Raines, R. T. Thioamides in the collagen triple helix. *Chem. Commun.* **2015**, *51*, 9624−9627.

(3) Stewart, W. E.; Siddall, T. H. Nuclear magnetic resonance studies of amides. *Chem. Rev.* **1970**, *70*, 517−551.

(4) Sandström, J.; Uppström, B. NMR spectra and conformations of some simple N-methyl thioamides. *Acta Chem. Scand.* **1967**, *21*, 2254−2260.

(5) (a) Wiberg, K. B.; Rush, D. J. Solvent effects on the thioamide rotational barrier: An experimental and theoretical study. *J. Am. Chem. Soc.* **2001**, *123*, 2038−2046. (b) Wiberg, K. B.; Rablen, P. R. Why Does Thioformamide have a larger rotational barrier than formamide? *J. Am. Chem. Soc.* **1995**, *117*, 2201−2209.
(6) Zhang, J.; Liu, Z.; Yin, Z.; Yang, X.; Ma, Y.; Szostak, R.; Szostak, M. Preference of Z-Thioamide Structure in N-Thioacyl-N-methylanilines. *Org. Lett.* **2020**, *22*, 9500−9505.
(7) Ruud, K.; Helgaker, T.; Bak, K. L.; Jørgensen, H. J. A. Jensen, Hartree-Fock Limit Magnetizabilities from London Orbitals. *J. Chem. Phys.* **1993**, *99*, 3847−59.
(8) Bordwell, F. G.; Ji, G. Z. Effects of structural changes on acidities and homolytic bond dissociation energies of the hydrogen-nitrogen bonds in amidines, carboxamides, and thiocarboxamides. *J. Am. Chem. Soc.* **1991**, *113* (22), 8398−8401.
(9) Olmstead, W. N.; Margolin, Z.; Bordwell, F. G. Acidities of water and simple alcohols in dimethyl sulfoxide solution. *J. Org. Chem.* **1980**, *45*, 3295−3299.
(10) Smiszek-Lindert, W.; Nowak, M.; Kusz, J. *Acta Crystallogr., Sect. E: Struct. Rep. Online* **2007**, *63*, No. o3917.
(11) Maeda, H.; Kamijo, N.; Fukui, K. *Cryst. Struct. Commun.* **1976**, *5*, 129.
(12) Zhao, G. *Acta Crystallogr., Sect. E: Cryst. Commun.* **2015**, *71*, No. o353.
(13) Hyodo, T.; Kawahata, M.; Hikami, Y.; Komatsu, A.; Tominaga, M.; Yamaguchi, K. Cycloalkanes and cycloalkenes in dispersive force. *CrystEngComm* **2019**, *21*, 1548−1554.
(14) Tominaga, M.; Hyodo, T.; Maekawa, Y.; Kawahata, M.; Yamaguchi, K. One-Step Synthesis of Cyclophanes as Crystalline Sponge and Their [2]Catenanes through SN_{Ar} Reactions. *Chem. - Eur. J.* **2020**, *26*, 5157−5161.
(15) Haisa, M.; Kashino, S.; Ueno, T.; Shinozaki, N.; Matsuzaki, Y. *Acta Crystallogr., Sect. B: Struct. Crystallogr. Cryst. Chem.* **1980**, *36*, 2306.
(16) Saito, S.; Toriumi, Y.; Tomioka, N.; Itai, A. Theoretical Studies on *cis*-Amide Preference in *N*-Methylanilines. *J. Org. Chem.* **1995**, *60*, 4715−4720.
(17) Pros, G. J.; Bloomfield, A. J. Why Do *N*-Alylated Anilides Bend Over? The Factors Dictating the Divergent Conformational Preferences of 2° and 3° *N*-Aryl Amides. *J. Phys. Chem. A* **2019**, *123*, 7609−7618.
(18) Wang, L.; Friesner, R. A.; Berne, B. J. Replica Exchange with Solute Scaling: A More Efficient Version of Replica Exchange with Solute Tempering (REST2). *J. Phys. Chem. B* **2011**, *115*, 9431−9438.
(19) Roos, K.; Wu, C.; Damm, W.; Reboul, M.; Stevenson, J. M.; Lu, C.; Dahlgren, M. K.; Mondal, S.; Chen, W.; Wang, L.; Abel, R.; Frisner, R. A.; Garder, E. D. OPLS3e: Extending Force Field Coverage for Drug-Like Small Molecules. *J. Chem. Theory Comput.* **2019**, *15*, 1863−1874.
(20) (a) Cohn, J. Theory of the Radial Distribution Function. *J. Phys. Chem.* **1968**, *72*, 608−616. (b) Kopera, B. A. F.; Retsch, M. Computing the 3D Radial Distribution Function from Particle Positions: An Advanced Analytic Approach. *Anal. Chem.* **2018**, *90*, 13909−13914.
(21) Hollosi, M.; Majer, Z.; Zewdu, M.; Ruff, F.; Kajtar, M.; Kövér, K. E. Mixed intramolecular H-bonds of secondary thioamides. *Tetrahedron* **1988**, *44*, 195−202.
(22) (a) Bader, R. F. W. Atoms in Molecules. *A Quantum Theory*; Oxford University Press: New York, 1990. (b) Runtz, G. R.; Bader, R. F. W.; Messer, R. R. Definition of bond paths and bond directions in terms of the molecular charge distribution. *Can. J. Chem.* **1977**, *55*, 3040−3045. (c) Matta, C. F.; Boyd, R. J. *The Quantum Theory of Atoms in Molecules: From Solid State to DNA and Drug Design*; Wiley-VCH: New York, 2007. (d) Bader, R. F. W. Bond Paths Are Not Chemical Bonds. *J. Phys. Chem. A* **2009**, *113*, 10391−10396. (e) Zhai, L.; Otani, Y.; Ohwada, T. Uncovering the Networks of topological Neighborhoods in β-strand and Amyloid β-sheet structures. *Sci. Rep.* **2019**, *9*, 10737. (f) Lammertsma, K.; Ohwada, T. Three-Center, Two-Electron Systems. Origin of the Tilting of Their Substituents. *J. Am. Chem. Soc.* **1996**, *118*, 7247−7254.
(23) (a) Naruse, Y.; Ma, J.; Takeuchi, K.; Nohara, T.; Inagaki, S. π-Relaxation of the ring strain: design of polycyclic unsaturated silicon molecules. *Tetrahedron* **2006**, *62*, 4491−4497. See also references cited therein. (b) Inagaki, S. *Orbital in Chemistry*; Springer: Heidelberg, 2009.
(24) Takahashi, Y.; Ikeda, H.; Kanase, Y.; Makino, K.; Tabata, H.; Oshitari, T.; Inagaki, S.; Otani, Y.; Natsugari, H.; Takahashi, H.; Ohwada, T. Elucidation of the E-Amide Preference of N-Acyl Azoles. *J. Org. Chem.* **2017**, *82*, 11370−11382.
(25) Charette, A. B.; Grenon, M. Mild Method for the Conversion of Amides to Thioamides. *J. Org. Chem.* **2003**, *68*, 5792−579.
(26) Otsuka, R.; Maruhashi, K.; Ohwada, T. Latent Bronsted Base Solvent-Assisted Amide Formation from Amines and Acid Chlorides. *Synthesis* **2018**, *50*, 2041−2057.
(27) *Gaussian 16*, Revision C.01; Frisch, M. J.; Trucks, G. W.; Schlegel, H. B.; Scuseria, G. E.; Robb, M. A.; Cheeseman, J. R.; Scalmani, G.; Barone, V.; Petersson, G. A.; Nakatsuji, H.; Li, X.; Caricato, M.; Marenich, A. V.; Bloino, J.; Janesko, B. G.; Gomperts, R.; Mennucci, B.; Hratchian, H. P.; Ortiz, J. V.; Izmaylov, A. F.; Sonnenberg, J. L.; Williams-Young, D.; Ding, F.; Lipparini, F.; Egidi, F.; Goings, J.; Peng, B.; Petrone, A.; Henderson, T.; Ranasinghe, D.; Zakrzewski, V. G.; Gao, J.; Rega, N.; Zheng, G.; Liang, W.; Hada, M.; Ehara, M.; Toyota, K.; Fukuda, R.; Hasegawa, J.; Ishida, M.; Nakajima, T.; Honda, Y.; Kitao, O.; Nakai, H.; Vreven, T.; Throssell, K.; Montgomery, J. A., Jr.; Peralta, J. E.; Ogliaro, F.; Bearpark, M. J.; Heyd, J. J.; Brothers, E. N.; Kudin, K. N.; Staroverov, V. N.; Keith, T. A.; Kobayashi, R.; Normand, J.; Raghavachari, K.; Rendell, A. P.; Burant, J. C.; Iyengar, S. S.; Tomasi, J.; Cossi, M.; Millam, J. M.; Klene, M.; Adamo, C.; Cammi, R.; Ochterski, J. W.; Martin, R. L.; Morokuma, K.; Farkas, O.; Foresman, J. B.; Fox, D. J. Gaussian, Inc., Wallingford, CT, 2016.
(28) Baerends, E. J. et al. *ADF2020. Theoretical Chemistry*; Vrije Universiteit: Amsterdam, The Netherlands, 2020, http://www.scm.com. te Velde, G.et al.Chemistry with ADF*J. Comput. Chem.* **2001**, *22* 931−967.

https://doi.org/10.1021/acs.joc.1c00801
J. Org. Chem. XXXX, XXX, XXX−XXX